




Cite this: *Mater. Adv.*, 2024,  
5, 4974

Received 6th February 2024,  
Accepted 26th April 2024

DOI: 10.1039/d4ma00120f

rsc.li/materials-advances

# Insight into aligned nanofibers improving fuel cell performances: strategies, rationalities, and opportunities

Muhammad Yusro <sup>\*ab</sup> and Viktor Hacker <sup>a</sup>

Nanofibers are advanced materials widely used in fuel cell applications owing to their superior characteristics of large surface area and porosity. Aligned nanofibers, a next-level development in nanofibers, is a promising approach for implementation in fuel cell applications, considering that they enhance specific properties compared to randomly orientated structures. This review presents the current strategies for fabricating aligned nanofibers and explores various methods to obtain targeted assemblies. These methods include increasing the speed of the rotating collector, applying multiple electric fields, and using engineering-defined collectors, for instance, wiring drums, patterned strips, frame shapes, rotating discs, rotating jets, and guide column arrays. Moreover, the rationality behind why this structure can improve fuel cell performance is elaborated, which includes enhanced conductivity, improved mass transport, structural durability, and reduced water flooding. The prospects and challenges of implementing aligned nanofibers in fuel cells are also included.

## 1. Introduction

Human civilization has always been dependent on energy. Before the industrial revolution, people used wood as an energy source to satisfy their basic needs. Initiated by James Watt with his steam engine in 1769, most energy services in recent centuries have been provided by fossil fuels.<sup>1</sup> However, the use of fossil fuels is not sustainable, given that it results in an increase in the carbon dioxide content in the atmosphere, which has already significantly impacted the climate. This condition is a pressing issue that requires urgent attention. Therefore, new approaches for environmentally friendly energy production are urgently needed as a policy to decarbonize energy systems and consequently strengthen regional energy independence through the use of renewable energy sources.<sup>2</sup>

Hydrogen has the advantage of availability compared to other renewable resources. Mainly, natural resources cannot be controlled by humans; often, the sun does not shine, or the wind does not blow during specific periods. Alternatively, hydrogen can be a stable resource because it does not directly depend on natural phenomena, providing continuous energy storage to supply power.

One of the devices that employs hydrogen as an energy source is the fuel cell. This technology applies reverse electrochemical principles to generate electrical current. The inlet used in a fuel cell depends on the type of fuel cell. Generally, the different types of fuel cells have hydrogen on the anode side and oxygen on the cathode side. Compared to other electrochemical technology devices, for instance, batteries, where electricity is produced from internal energy, fuel cell technology has substantial benefits, especially the reactants can be continuously charged.<sup>3</sup> Moreover, the electrodes in fuel cells are catalytic and relatively stable. Additionally, their operation can be sustained if the flow is continuously maintained. From an ecological perspective, fuel cells produce water and steam as their product, making these devices a promising approach from an environmental perspective compared to fossil fuel, which produces carbon excess.

It has been reported that the use of nanofibers is a promising approach to enhance the performance of fuel cells. Nanofibers are nanomaterials that have the shape of fibres defined by dimensions in the range of 50–500 nm.<sup>4</sup> Owing to these properties, nanofibers can act as membranes with large porosity and surface area. In fuel cell applications, this advanced material successfully upgrades the quality of the product compared to conventional methods such as solution casting.<sup>5</sup>

Nanofibers can act as a membrane providing proton or anion transfer to the other electrode, enhancing this feature. The prime characteristics of nanofibers applied in fuel cells are providing high surface area and porosity and promoting the

<sup>a</sup> Institute of Chemical Engineering and Environmental Technology,  
Graz University of Technology, Inffeldgasse 25/C, 8010 Graz, Austria.  
E-mail: yusro@student.tugraz.at

<sup>b</sup> Institut Teknologi Telkom Purwokerto, Jalan D.I. Panjaitan 128, Purwokerto,  
53147, Indonesia



establishment of interconnected networks.<sup>4</sup> This structure has been reported to have an impact on the performance of fuel cells in terms of preventing their electrochemical degradation<sup>4</sup> and facilitating better catalytic performances,<sup>6</sup> high stability under repeated cycling,<sup>7</sup> and high efficiency in the hydrogen evolution reaction,<sup>4</sup> acting as highly efficient and stable bifunctional electrocatalyst for water splitting,<sup>4</sup> and enhancing hydroxide conduction.<sup>4</sup>

The first article related to aligned nanofibers was published in 1993, when Doshi and Reneker reported that an increase in the electric potential can make fibres more oriented in poly(ethylene oxide).<sup>8</sup> Since then, strategies to align nanofibers have been continuously developed, with several new approaches reported to date. For instance, rotating disc method,<sup>9</sup> use of multiple electric fields,<sup>10</sup> tuning the shape of the frame,<sup>9</sup> using patterned electrodes,<sup>11</sup> rotating jets,<sup>12</sup> and guiding column arrays,<sup>13</sup> and increasing the speed of the drum collector<sup>14</sup> have been reported for the successful fabrication of oriented nanofibers.

Aligned nanofibers have superior characteristics compared to random structures. Consequently, the advantages of these structures facilitate enhanced mass transport,<sup>15</sup> electrochemical activity,<sup>16</sup> mechanical integrity (durability),<sup>17</sup> and electrical conductivity.<sup>18</sup> The experimental results provided by characterization support the use of aligned nanofibers.

However, although the nanofiber approach has promising prospects in enhancing the performance of fuel cells, it still needs to be fully exploited to implement oriented nanofibers in fuel cell applications. The research and development of aligned nanofibers for fuel cell applications are still in their infancy. Nonetheless, this strategy can potentially be employed to develop membrane electrode assemblies (MEA) for fuel cell applications.

This review aims to present insight into the use of aligned nanofibers as one prospective strategy for the performance of

improving fuel cells. The outlook of this review includes the strategies to fabricate aligned nanofibers, the rationality of the performance of fuel cells and their characterization, and finally the opportunities regarding future research and challenges in fuel cells.

## 2. Fuel cells

Fuel cells are devices based on the electrochemical principle to convert chemical energy to electrical energy. This process is continuous if fuel and an oxidant are supplied. For instance, in the proton exchange membrane fuel cell (PEMFC), hydrogen ( $H_2$ ) gas is supplied to the anode (–). Meanwhile, oxygen is supplied to the cathode (+). At the anode, the  $H_2$  molecule splits into two protons and two electrons by the catalytic process. The protons infiltrate the membrane, and the electron flows through the wire, producing an electrical current. Furthermore, proton particles linked with electrons and oxygen form water at the cathode.

Regarding fuel cell development, the type of fuel cell can be classified according to the applied electrolyte.<sup>19</sup> To date, at least six types of fuel cells have been established, which are polymer electrolyte fuel cell (PEFC), alkaline fuel cell (AFC), direct alcohol fuel cell (DAFC), phosphoric acid fuel cell (PAFC), molten carbonate fuel cell (MCFC), and solid oxide fuel cell (SOFC).<sup>20–22</sup> Fig. 1 illustrates the mechanism of the various types of fuel cells.

It has been recognized that PEMFC/PEFC is the leading fuel cell technology due to its characteristics such as high-power density, low weight, and ability to operate at low temperatures (typically at around 80 °C).<sup>23</sup> Nonetheless, this type of fuel cell has significant challenges, mainly it employs an expensive catalyst (platinum).<sup>24</sup> Thus, to address these limitations, an anion exchange membrane (AEM) can be employed, considering



Fig. 1 Illustration of the structure and mechanism of various types of fuel cells.



its advantage that it avoids the use of expensive metal catalysts. Moreover, this approach reduces the severe corrosion under alkaline conditions due to the counter-direction between the fuel and OH ions. However, although AEM shows significant promise to overcome the issues associated with PEM, this type of fuel cell must be managed regarding its excessive water absorption, poor mechanical properties, membrane swelling, poor ion conductivity, and poor membrane stability.<sup>25</sup> Another promising candidate is the direct alcohol fuel cell (DAFC). This structure is similar to PEMFC. When methanol is used in the fuel in a DAFC uses, it is called a direct methanol fuel cell (DMFC). This is because this fuel can be directly used as the fuel source without a reforming process, and this type of fuel cell has a more compact system regarding its structure and provides a higher energy density.<sup>19</sup> PAFC utilizes liquid phosphoric acid and ceramic electrolytes such as silicon carbide or glass mat as membranes.<sup>26</sup> This type of fuel cell also employs platinum as a catalyst. Regarding efficiency, the efficiency of PAFC is comparable to that of PEMFC. Nonetheless, this type of fuel cell works at higher temperatures to manage the fuel cell impurities. PAFC is usually applied in stationary applications, satisfying a high energy demand. SOFC employs a ceramic material as the electrolyte membrane. This type of cell operates at 1800 degrees Fahrenheit, making it the highest-temperature fuel cell.<sup>27</sup> Compared to the above-mentioned fuel cells, this type of fuel cell does not use platinum-based materials as a catalyst. SOFC is considered to use internal reformation and commonly used natural gas as fuel. Another type of fuel cell that operates at high temperatures and uses non-platinum catalysts through internal reforming is MCFC. This type of fuel cell utilizes molten carbonate salt as a membrane electrolyte,<sup>28</sup> reducing the cost. Also, its high working temperature can reduce the requirement of a costly metal catalyst, reducing the cost compared to the fuel cells that use precious materials.

Regarding the structure of fuel cells, they are constructed using several components with distinct materials. From outside to inside, these components include bipolar plates, gaskets,

gas diffusion layers (GDL), catalyst layers (CL), and membranes. However, all these components or layers can be degraded, resulting in a decline in the function and performance of fuel cells.<sup>29</sup>

Table 1 presents a summary of the risk factors and causes for the decline in the performance of fuel cells.

The first component, the membrane, is in the central part of the fuel cell structure. The role of the membrane is to ensure that only the required ions pass between the anode and cathode. A membrane is a particularly important material that manages to transfer only positively charged ions from the fuel and prevents the movement of electrons through the membrane structure. An excellent membrane in fuel cells should exhibit durability, chemical stability (against reactive radicals), high thermal stability, and mechanical stability (combat gas crossover).<sup>29</sup> In PEM fuel cells, it has been reported that mechanical degradation of the membrane structure is the main factor for their early-stage failure.<sup>31</sup>

The catalyst layer is a component placed on both sides of the membrane. One side functions as the anode, and the other side acts as the cathode. On the anode side, hydrogen molecules are split into protons and electrons. On the cathode side, water is produced by the reaction between oxygen and the protons generated by the anode. Several factors can damage the catalytic layer in fuel cells, for instance, higher voltages, humidity, and load cycling. Furthermore, in PEM, these factors lead to structural damage and accelerate corrosion.<sup>32</sup>

GDLs are structures located on the outside of the catalyst layers, which function to transport the reactants to the catalyst layer. This component also plays a role in removing water. In fuel cells, gases diffuse in the pores of the GDL, which is composed of a hydrophobic material to keep the pores open. It has the function of preventing the accumulation of excessive water. The GDL consists of two layers, a microporous layer and a macroporous layer. The macroporous layer facilitates an electrical and thermal pathway to the flow-field plates. Moreover, this structure enables the permeation of particles through

**Table 1** Risk factors and their causes in the components of fuel cells<sup>30</sup>

| Components of fuel cells | Risk factors                                                                                                                                                           | Causes                                                                                                                                                                                                                                                                           |
|--------------------------|------------------------------------------------------------------------------------------------------------------------------------------------------------------------|----------------------------------------------------------------------------------------------------------------------------------------------------------------------------------------------------------------------------------------------------------------------------------|
| Membrane                 | Mechanical degradation<br>Thermal degradation<br>Chemical electrochemical degradation<br>Membrane thinning<br>Pinhole formation                                        | Mechanical stress caused by non-uniform pressure<br>Thermal stress caused by non-uniform temperature<br>Contamination, radical exposure<br>Chemical degradation, high temperature<br>Mechanical tension, accelerated by low and alternating humidification and high temperatures |
| Catalyst layer           | Decrease in mass transport rate of the reactant<br>Loss of conductivity<br>Loss of activation<br>Loss of tolerance<br>Decrease in water management<br>Carbon corrosion | Mechanical stress<br>Corrosion<br>Sintering or dealloying<br>Contamination<br>Hydrophobicity change<br>Fuel starvation, high humidity, quick high load charges                                                                                                                   |
| Gas diffusion layer      | Decreased ability in water management<br>Decrease in mass transport<br>Conductivity loss                                                                               | Mechanical stress and change in material hydrophobicity<br>Degradation of backing material<br>Corrosion                                                                                                                                                                          |
| Gasket                   | Mechanical failure                                                                                                                                                     | Corrosion<br>Mechanical stress                                                                                                                                                                                                                                                   |
| Bipolar plate            | Fracture/deformation<br>Loss of conductivity                                                                                                                           | Corrosion<br>Mechanical stress<br>Corrosion and oxidation                                                                                                                                                                                                                        |



its macroscopic layer. The microscopic layer manages water, reducing the thermal and electrical contact near the catalyst layer. It has been mentioned that a significant issue in this structure is the hydrophobicity changes on its surface and porous layer caused by degradation.<sup>33</sup>

The main function of the gasket is to distribute continuous pressure and reduce contact with the components inside the fuel cell. It also secures the gas in a seal-tight condition. This component plays a significant role in the durability of the fuel cell. Thus, the gasket is usually built using a rubbery polymer.<sup>34</sup>

Bipolar plates have the function of providing electrical conduction between cells. They also provide physical strength to the stack. Bipolar plates have a surface constructed by channels, which allow gases to enter the structures. It has been reported that metallic bipolar plates are recommended due to their small dimensions and weight. Bipolar plates are required to protect against corrosion and enable long-term operation.<sup>29</sup> Table 1 presents the risk factors and their causes in the components of fuel cells, which refers to.<sup>30</sup>

### 3. Electrospinning

Electrospinning is the most recommended method for the fabrication of nanofibers because of its versatility. This apparatus can be used on the lab and industrial scales and can mix various materials (composites and additives) to achieve the required targeted properties. Electrospinning systems consist of a pump, syringe, polymer solution, needle as a tip, high voltage, and collector. This system applies electrostatic force to stretch and elongate the fibre. This electrostatic force should be sufficient to form a Taylor cone at the tip of the needle due to its positive charge and strong enough to pull out the solution and move it to the collector. During this movement, the solute

evaporates, and the fibre gets thinner and thinner until it reaches nanometre dimensions. The source of the electrostatic force comes from a high-voltage power supply.

The mechanism of this instrument is that positive charge is converged in a formed Taylor cone, acting as an anode that supplies a high voltage power and gets repelled to the collector, which acts as the cathode. This system could produce three structures, namely, nanofibers, nanobeads, and droplets.

These three varieties originate from the interaction among the parameters influencing the process. At a certain distance, this phenomenon causes the polymer jet to the grounded collector. The jet is a straight line in a short distance because of the jet effect. However, in the next event, the fibre becomes thinner and smoother due to the evaporation of the solute polymer. In this line, the interaction between the fibre, which is charged, and the air occurs, creating a non-woven polymer fibre.

Fig. 2 illustrates the related parameters in the electrospinning process, which depend on or influence each other. From an experimental viewpoint, the events in electrospinning have been examined and influenced by the parameters affected by the electrostatic forces, which lead to successful or failed products. The parameters can be classified into three categories, including fluid parameters, set-up parameters, and ambient parameters. Among these three parameters, the fluid factor consists of viscosity, conductivity, and surface tension, which is the most influential parameter, and thus must be appropriately considered.<sup>35</sup>

Firstly, viscosity is the parameter that can affect the size and shape of the fibre product. This parameter is an important factor in the fabrication process, which can lead to the presence of solution in the fibre. If the viscosity is not high enough, the stretching and elongating process tends to form beads or a spray. Viscosity is related to the concentration of the material solution. Thus, the solvent can also lead to different viscosities.

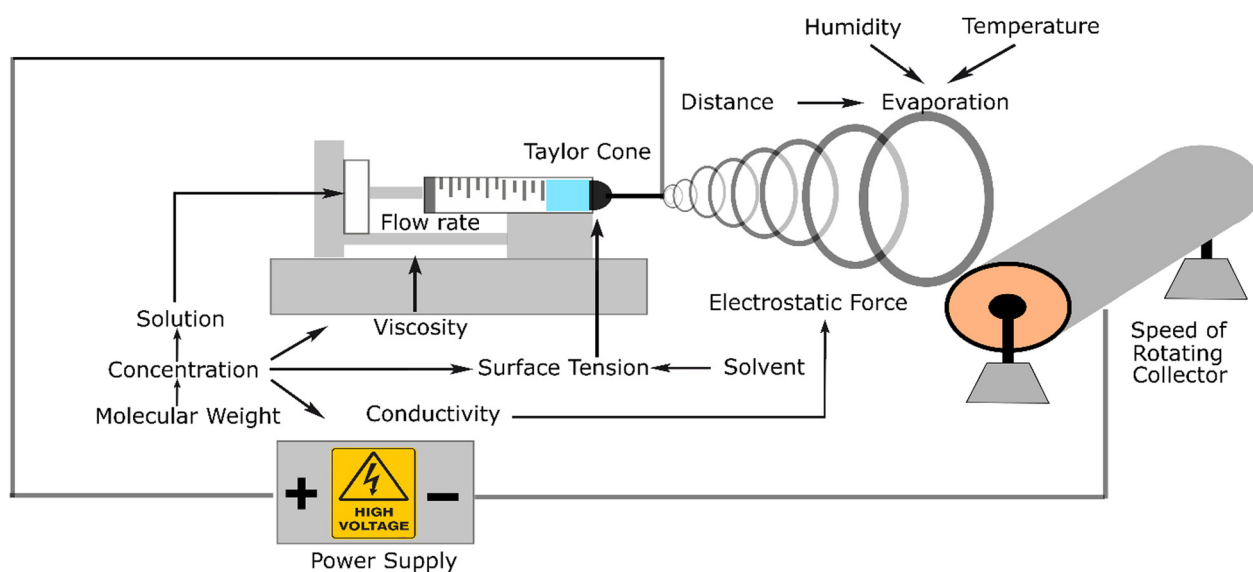


Fig. 2 Illustration of the devised parameters in the electrospinning process.



The second parameter, conductivity, is related to the positive charge that appears in the solution. The higher the conductivity, the stronger the force in the system. For instance, chitosan exhibits high conductivity with an increase in its concentration. Accordingly, an additional material is required to counter this high conductivity.

The last surface tension parameter affects the Taylor cone, which initiates the process of elongating and stretching the nanofiber. The surface tension is affected by the solvent; it has been reported that a low surface tension increases the failure of nanofiber fabrication. It has been mentioned that in the process of electrospinning, an electrostatic force is applied. The positive charge that converges in the tip forms a Taylor cone, acting as the anode that comes from a high-voltage power supply and gets repelled by the collector, which acts as the cathode. The result of this system can be three structures, namely nanofibers, nanobeads, and droplets. These three varieties originate from the interaction between the influencing parameters.

The devised parameters in the system interact with each other, determining whether a nanofiber is created or not. Based on their source, the parameters can be classified into three main categories, which are fluid parameters, set-up parameters, and environment parameters. Each category has sub-categories that affect the fabrication process.

Table 2 presents the effect of the electrospinning parameters on the size of the fibres. The diameter of the nanofiber reportedly can affect the performance of fuel cells.<sup>36,37</sup> It is also interesting to explore the relationship between the geometrical aspect and the fuel cell performance by modulating the influencing parameters.

## 4. Strategies for the fabrication of aligned nanofibers

The fabrication of aligned nanofibers requires a strategy that typically adds special geometrical apparatus to the collector. This approach enables the nanofiber to sit more oriented as soon as it falls on the collector. Interestingly, not only one directional aligned material can be fabricated with electrospinning, but it has been established that by designing a specific patterned strip that has conductive properties,<sup>57</sup> two strip directions with two and three axial nanofiber structures can be formed using this electrospinning method. Fig. 3 illustrates the current strategies employed to fabricate aligned nanofibers.

### 4.1. Increasing the speed of rotating collector

The simplest way to fabricate aligned nanofibers is by increasing the speed of the rotary drum collector. Numerous reports show that this strategy can be employed to successfully fabricate uni-axial nanofibers. It has been reported that a speed in the range of 800–5000 rpm is applied.<sup>18,61</sup> The various materials that have been successfully transformed into aligned nanofibers include poly(vinyl alcohol) (PVA),<sup>14</sup> metal–organic frameworks (MOFs),<sup>18</sup> poly( $\epsilon$ -caprolactone) (PCL),<sup>62,63</sup> sulfonated poly(phthalazone ether sulfone ketone) (SPPEK),<sup>17,18</sup> chitosan (Cs),<sup>61</sup> poly(ethylene oxide) (PEO),<sup>61</sup> and polyacrylonitrile (PAN).<sup>64</sup>

It has been noted that increasing the speed of the rotating collector reduces the size of the nanofiber. This phenomenon is attributed to the fact that increasing the speed of the collector will enhance the applied stretching force in the nanofiber

**Table 2** Electrospinning parameters and the effect of their modulation on the size of nanofibers

|         | Parameters                                      | Effect                                                                                                                                                              |                                                                                                                                  | Ref.            |
|---------|-------------------------------------------------|---------------------------------------------------------------------------------------------------------------------------------------------------------------------|----------------------------------------------------------------------------------------------------------------------------------|-----------------|
|         |                                                 | Increase                                                                                                                                                            | Decrease                                                                                                                         |                 |
| Set up  | Flow rate                                       | Decreasing the fibre size. Too high flow rate causes the Taylor cone to swell (droplet).                                                                            | Increasing the fibre size. Too low flow rate causes the solution to retreat into the nozzle (unformed Taylor cone).              | 38–42           |
|         | Voltage                                         | Increasing the conic angle and decreasing the fibre size result in a smaller Taylor cone, smaller pores, multiple jets, and formation of beads (very high voltage). | Enormous Taylor cone, increase in fibre size, resulting in more prominent pores. Too low applied voltage prevents jet formation. | 38,40, 42–44    |
|         | Distance tip to the collector                   | Decreasing the fibre size due to evaporation.                                                                                                                       | Decrease in distance causes an increase in electrical force (a minimum distance is required).                                    | 40,44–46        |
|         | Rotating collector speed                        | Aligned nanofiber formation.                                                                                                                                        | Isotropic nanofiber formation.                                                                                                   | 17,47,48        |
| Fluid   | Viscosity (corresponds to concentration and MW) | Increasing fibre dimensions smoothens the fibre (less beads); a highly viscous solution cannot be injected from the nozzle.                                         | Decreasing fibre size, smaller pores and shallow value generate beads.                                                           | 38,41,46, 49–51 |
|         | Conductivity                                    | Higher conductivity increases the limitation of fabrication.                                                                                                        | Minimum conductivity is necessary for the electrospinning process.                                                               | 35,44           |
|         | Surface tension                                 | Higher surface tension results in droplets.                                                                                                                         | Very low surface tension results in the formation of droplets.                                                                   | 44,52           |
| Ambient | Temperature                                     | Higher temperature decreases the nanofiber size.                                                                                                                    | Higher temperature increases the nanofiber size.                                                                                 | 53–56           |
|         | Humidity                                        | Higher humidity increases the nanofiber size and the instability of the fiber.                                                                                      | Lower humidity permits faster solvent evaporation.                                                                               | 54–56           |





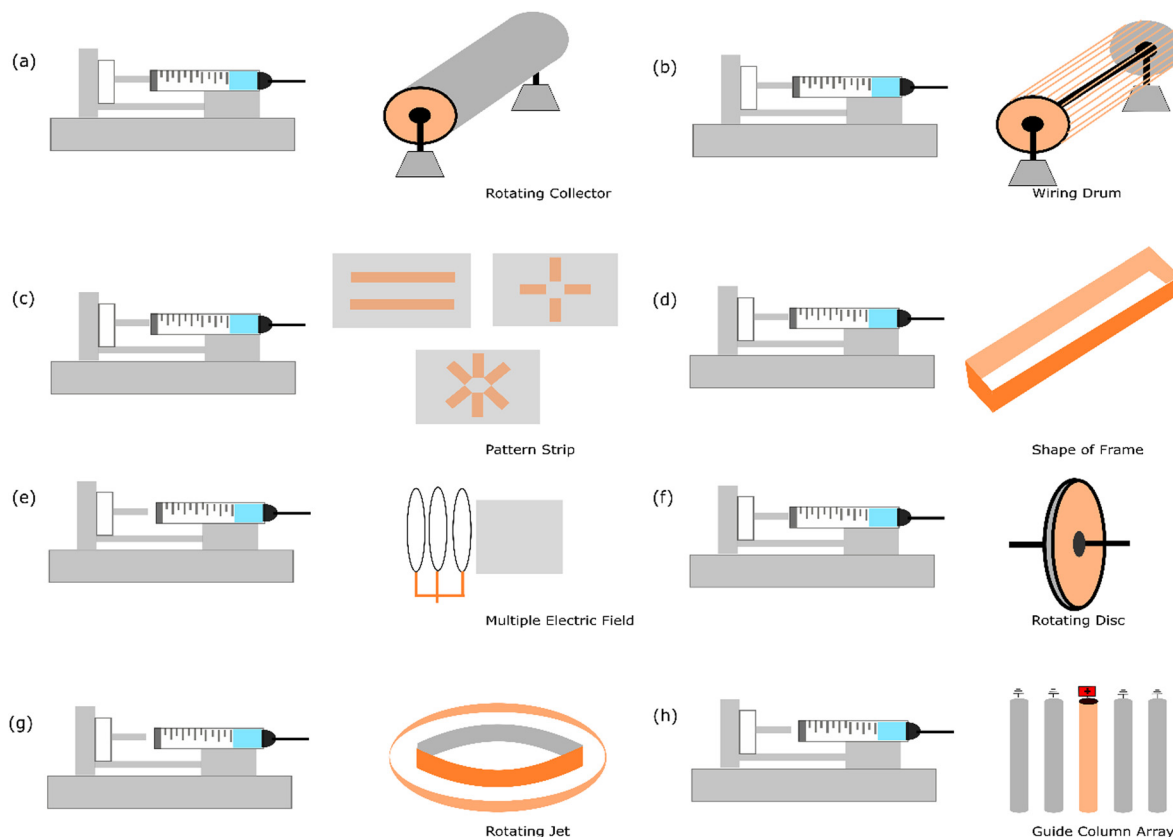


Fig. 3 Illustration of the current methods for aligning nanofibers using electrospinning: (a) increasing the speed of the rotating collector,<sup>14</sup> (b) wiring drum,<sup>58</sup> (c) patterned strip,<sup>57</sup> (d) shape of frame,<sup>59</sup> (e) multiple electric fields,<sup>10</sup> (f) rotating disc collector,<sup>9</sup> (g) rotating jet,<sup>60</sup> and (h) guide column array.<sup>13</sup>

induced by the high-speed rotating drum.<sup>14</sup> An interesting result has also been published that by increasing the drum speed (800 to 2500 rpm), the modulus also increases ( $3.83 \pm 0.70$  to  $41.32 \pm 1.64$ ) in the parallel nanofiber.<sup>61</sup> Regarding the orientation, it has been found that by increasing the speed of the collector gradually, notably 1.000 rpm, 1.500 rpm, 2.000 rpm, and 2.500 rpm, the geometrical angle in the range of 10–0° changes be about 35%, 52%, 57%, and 73%, respectively. This result indicates that the alignment of the nanofibers improves considerably with an increase in the rotary speed.<sup>65</sup>

#### 4.2. Wiring drum

A wiring drum is a modified rotating collector with parts like a wire similar to a yarn spinner. Theoretically, with these customized structures, the fibre that falls onto the rotating drum can be easily placed constantly, avoiding a random orientation. It has been reported that Nylon-6 was successfully fabricated into an aligned nanofiber using this method.<sup>58</sup>

It has been reported that this technique is robust and can be easily collected without breaking the oriented structure. This experiment used copper wires spaced uniformly in a circular drum formation, which functioned as a collector. This experiment also noted that a proper alignment is achieved in around 15 min of electrospinning, and after that, the fibres begin to condense and entangle. Nonetheless, the process of electrospinning for up to 40 min still produced an aligned structure.

#### 4.3. Patterned strip

In this strategy, two electrodes that can manage the fibre orientation are placed in the plane collector. Metal plates such as aluminum,<sup>66</sup> gold,<sup>57</sup> and copper<sup>67</sup> and conductive silicon<sup>68</sup> can be used to build this upgraded collector. It has been reported that this strategy is implemented in proton exchange membranes using sulfonated polyimide material.<sup>69</sup> The result of this approach is a one-strip nanofiber alignment.

An excellent feature of this strategy is that this plate can be customized given that the electrode is a patterned formation. By making various patterns, the geometry of the nanofiber can be engineered according to the desired goal. It has been reported that poly(vinylpyrrolidone) could be fabricated to become more than uni-axial nanofiber structures using this strategy. This approach is very promising for exploring more comprehensive variables regarding the effect of nanofiber geometry.<sup>57</sup>

#### 4.4. Shape of frame

The idea behind making frames with a specific shape is to control the deposition process when a fibre is deposited on the collector. When the fibre is deposited at a specific side of the frame, the continued fibre formation must be deposited at the other side. This process can make fibre aligned and uni-axially oriented. The different designs of the frame can be based on



different geometrical shapes, such as elliptical frame<sup>59</sup> and using two strips with an inclined gap.<sup>70</sup>

Due to the presence of two strips or sides configured to create a gap between the deposited side of the nanofiber, the nanofiber product is sequentially deposited across the edges of these two sides in an oriented formation. The materials used and successfully reported using this strategy are polycaprolactone,<sup>70</sup> polyamide-6,<sup>59</sup> and polylactide.<sup>59</sup>

#### 4.5. Multiple electric fields

The electric field is one of the parameters in the electrospinning process. It causes the elongated fibre to stretch from the tip to the collector. Normally, this process is formed by a random nanofiber formation. Alternatively, multiple electric fields need to be managed to transform the geometrical shape into a more oriented nanofiber. Simulation has reported that the electrospinning jet spins in the area between the tip and collector.<sup>71</sup> The modelling of the electrospinning process is necessary to solve the challenges in nanofiber production, particularly the whipping instability. This obstacle occurs in the chaotic oscillation of polymer jets, producing a random fibre formation.<sup>72</sup> In this case, an additional instrument needs to be placed at the appropriate distance.

Multiple electric fields using poly(ethylene oxide) material have been used in an experiment. The result showed that an aligned nanofiber was successfully fabricated. This experiment employed a secondary external field with the same polarity to manage the fibre formation. The controlled deposition of sub-micron polymer fibres (<300 nm in diameter) was enabled using an electrostatic lens element customised apparatus.<sup>10</sup>

#### 4.6. Rotating disc

It has been mentioned in the previous strategy that changing a flat collector to a rotating collector is one of the strategies to fabricate aligned nanofibers. However, the rotating drum is quite large regarding the area of deposition. In this case, the spun fibre affected by the electric field is not sufficiently elongated, and thus this strategy causes a slight angle in fibre formation. Accordingly, to solve this problem, an upgraded geometry needs to be developed with the idea of reducing the area of nanofiber placement in the rotating collector.

The rotating disc is a strategy that has a similar concept to the rotating collector but has a narrower area for nanofiber deposition. Hypothetically, when the fibre is placed in a small area (resembling the side of the disc), it can be directly rolled, creating a more oriented form. It has been reported that this strategy was successfully employed to form aligned nanofibers with a disc composed of aluminium. The geometrical design was 200 mm in diameter, and the thickness was only 5 mm. The material that was tested was polyethylene oxide.<sup>9</sup>

#### 4.7. Rotating jet

Another approach of modifying the collector in electrospinning is the method called rotating jet or centrifugal electrospinning, which is a technique inspired by the cotton candy production concept. This procedure implements a hollow metallic cylinder

as a collector with a needle placed in the centre of the cylinder. In this setup, parallel electrodes are inserted with a circular collector around the rotating spinneret, the needle tip acts as the positive electrode, and the collector acts as the negative electrode.<sup>73</sup> Due to the opposite charge between the collector and needle, repulsion is caused by the Coulomb force as the jet comes out of the rotating needle, and a nanofiber is formed in the inner surface of the cylinder. It has been reported that this method has advantages regarding high orientation over large collector areas.<sup>12</sup>

It has been reported that three parameters, including the solution properties,<sup>74</sup> operating parameters,<sup>75</sup> and mechanical objects of the device,<sup>76,77</sup> affect the morphology of the nanofibers fabricated by centrifugal spinning. Moreover, based on further study, the effects of surface tension, viscosity, speed of the spinneret, distance to the collector, evaporation rate, and diameter of the orifice on the morphology of the nanofibers are considered the most influencing parameters.<sup>75</sup>

#### 4.8. Guide column array

The guide column array was reported as a successful method to fabricate ceramic-based aligned nanofiber materials. The guide array was designed using copper tubing columns with a spacing of five 20 cm length, 0.5 cm diameter, and 2 cm apart.<sup>13</sup> A high-voltage power supply was applied to the centre column to generate electrostatic forces, while the remaining columns were grounded.

This method managed the electrospinning jet *via* electrostatic interactions between the electrified jet and the electrodes. By implementing an array of five conductive columns separated by an air gap, the electrified jet moves towards the guide column, and the repulsive coulomb forces deflect the fibre to the nearest grounded column.<sup>13</sup> In this event, the approaching fibre can disintegrate the charge. Subsequently, the dropped fibre is attracted to the central guide column *via* the same electrostatic forces that initially repelled it. The fibres could maintain a degree of polarization utilized in repelling due to the constant electric field between columns. It has also been found that the ceramic precursor solution conductivity is also correlated with the optimal operating voltage for the realization of aligned ceramic nanofibers.<sup>13</sup>

## 5. Rationality: effect of aligned nanofibers

Engineering nanofibers to be more aligned affects their properties related to fuel cell performances. The theoretical and experimental approaches for explaining why this profile enhances the characteristics of fuel cells will be elaborated in this part including enhanced conductivity, improved mass transport, structural stability, and reduced water flooding.

#### 5.1. Enhanced ion conductivity

Aligned nanofibers are promising to enhance the efficiency of fuel cells by improving the electrical conductivity and





Fig. 4 Comparison of the conductivity between aligned and non-aligned nanofiber or other conventional structures reported in the literature.

decreasing the electrical resistance due to the reduced tortuosity. It has been reported that sulfonated block copolymers, which have hydrophobic and hydrophilic parts, could be separated to the outside surface and the inside when fabricated as nanofibers *via* electrospinning.<sup>69,78</sup> This network provided a proton channel structure, which enhanced by the rapid transport of protons. Consequently, an excellent through-plane proton transport performance was observed in the fuel cell operation. Fig. 4 shows a comparison between the conductivity of aligned nanofibers and non-aligned nanofibers. Non-aligned nanofibers can be obtained by the solution casting method, which can be random nanofibers or without a nanofiber structure. This method has been successfully modelled using resistors, analogous to the study of fibre conductivity properties. The aligned nanofiber, which has an oriented structure, has superior conductivity, considering that its configuration is less of an obstacle to carrier transport to the other side. The prediction of the conductivity of nanofiber has also been modelled. This approach can approximate the fibre layering and swelling. In this model, the fibre network is considered a resistor and has been confirmed in proton and anion exchange membrane nanofiber-based fuel cell application.<sup>79</sup> The effect of aligned nanofibers in fuel cell applications has yet to be highly observed. Considering that this approach can theoretically and hypothetically increase the performance of fuel cells, this point of view is interesting to explore.

It has been reported that the ion conductivity increases when aligned nanofibers are implemented. An aligned nanofiber membrane composed of MOFs and SPPEK showed better

proton conductivity than the disordered membrane.<sup>18</sup> This report also mentioned that this type of nanofiber membrane has a higher conductivity value compared to the conventional method (solvent-casting). The proton conductivity reached  $(8.2 \pm 0.16) \times 10^{-2} \text{ S cm}^{-1}$  at 160 °C temperature operation under anhydrous condition. Moreover, in this study, the methanol permeability also reached up to  $0.707 \times 10^{-7} \text{ cm}^2 \text{ s}^{-1}$ , which is about 6% lower than that of Nafion-115.<sup>18</sup> Another study also reported that an aligned nanofiber could increase the conductivity. The proton conductivity showed a significantly higher value in the parallel direction.

Aligned nanofibers also increased the ion conductivity in an anion exchange membrane. The quaternized-poly(arylene ether sulfone) (Q-PAES) nanofibers fabricated using two strip electrodes were characterized to evaluate their anion conductivity. It was reported that regarding its conductivity, the oriented nanofiber showed a 10–15 times higher value. Based on the experimental data, the anion conductivity significantly increased from  $24 \text{ mS cm}^{-1}$  to  $140 \text{ mS cm}^{-1}$  (maximum) at an operating temperature of 90 °C for  $\text{OH}^-$  ion species.<sup>80</sup> Another study that used aligned nanofibers in anion membrane fuel cells also confirmed that the anion conductivity was successfully enhanced from  $0.9 \times 10^{-2}$  (80 °C) to  $1.81 \times 10^{-2}$  (80 °C).<sup>81</sup> The material used in this study was quaternized functional polyketone-based polyelectrolyte (QAFPK). Fig. 5 illustrates the idea of transforming a random nanofiber into an aligned nanofiber. Fig. 5(a) shows the implementation of aligned nanofibers in fuel cells as a membrane. Fig. 5(b) illustrates a comparison of





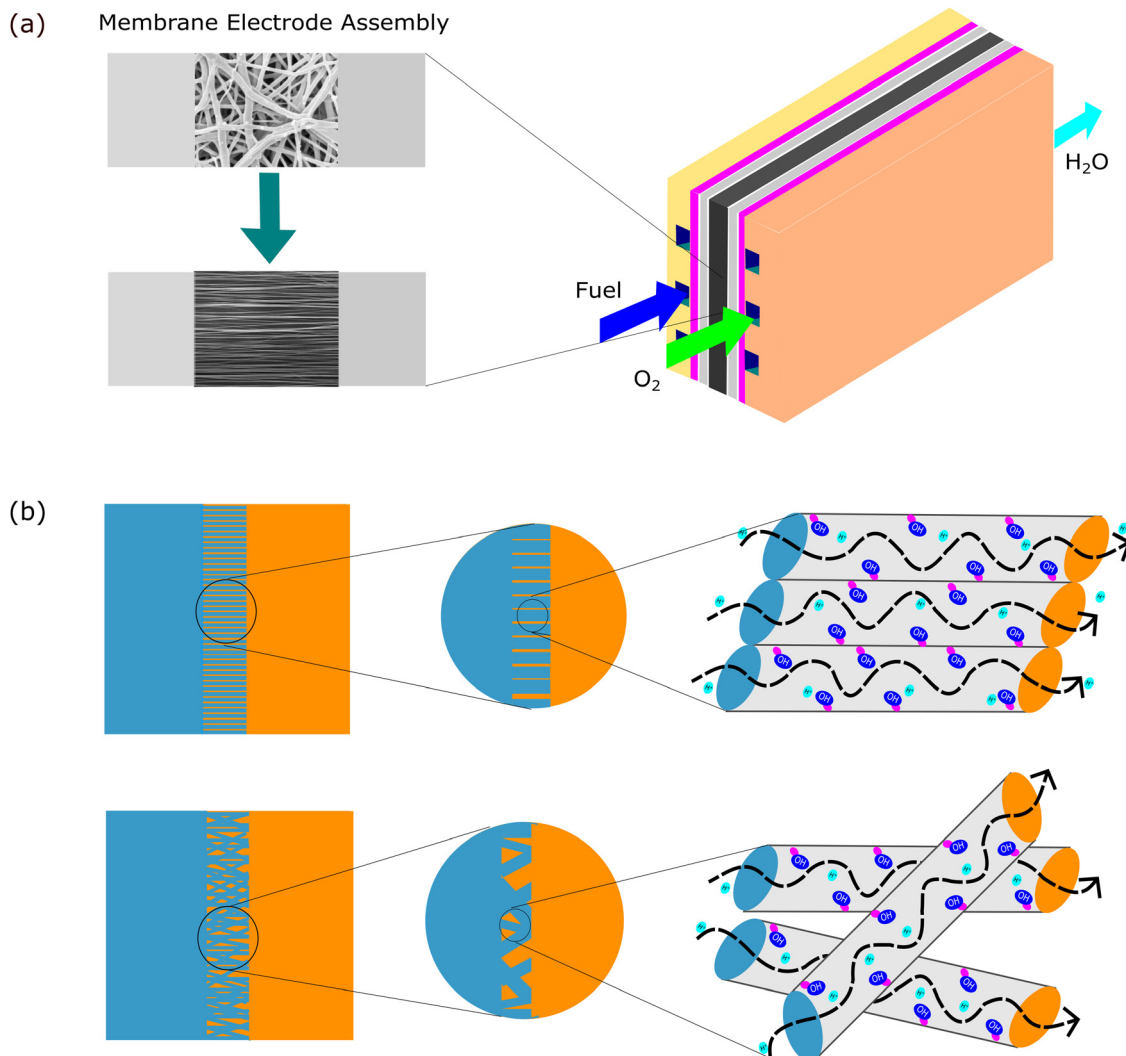


Fig. 5 (a) The idea of transforming a random nanofiber into an aligned nanofiber implemented in the membrane electrode assembly in fuel cells. (b) Comparison of aligned structures and isotropic fibres based on their transport function.

structure-oriented and isotropic membranes. It has been presented that the aligned nanofiber has a straightforward transport path, leading to higher conductivity.

## 5.2. Improved mass transport

Internal mass transfer limitations can be reduced by maximizing the porosity and lowering the tortuosity of the fibers.<sup>16</sup> In this case, an aligned structure leads to faster and more direct diffusion of species (improved mass transport kinetics). The aligned structure of nanofibers provides a better morphology and porosity-correlated membrane function, especially in terms of proton or ion transfer. Moreover, regarding polarity, a chaotic polarity distribution results in disordered mass transport; meanwhile, an oriented structure results in better transfer such as polar area for water transference and non-polar area for gas transport.<sup>15</sup> Fig. 6 shows an illustration of the comparison between disordered and oriented structures. Regarding electrodes, the nanofiber structure also provides clear pathways for

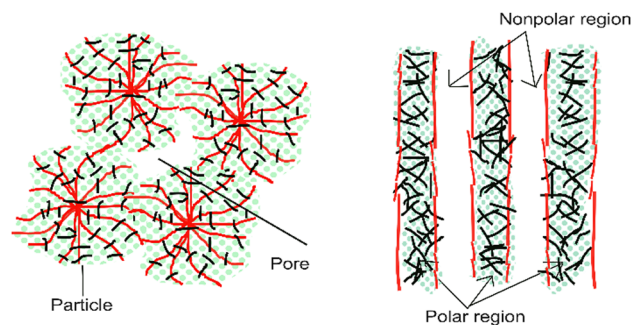


Fig. 6 Illustration of the polarity distribution between disordered (left) and more oriented nanofibers (right).<sup>15</sup>

the transport of the reactants and products within the fuel cell electrode. Furthermore, the surface area should be significant to host sufficient active sites per unit of volume.<sup>16</sup>

Regarding characteristics, ion exchange capacity is one of the properties of fuel cells that is correlated with mass



transport, specifically it is correlated with a specific number of ions available in the ion exchange process.<sup>82</sup> This characteristic represents the capacity of an insoluble functional group in the membrane to facilitate ion movement.<sup>83</sup> The method employed to determine the IEC is back titration.

It has been mentioned that ion exchange is correlated with the membrane properties, including the electrical resistance of the electrolyte, density of fixed charges in the membrane matrix and their distribution, permeability and selectivity of different ions in different membranes, the transport rate of water as a neutral component, stability regarding mechanical and chemical properties and the swelling in various electrolyte solutions.<sup>84</sup>

The ion exchange capacity is related to the anion conductive characteristic of nanofibers.<sup>85</sup> It has been reported that in a quaternized-poly(arylene ether sulfone) (Q-PAES) nanofiber, if the IEC value decreases, the anion conductivity also decreases. It has been tested that in the Q-PAES membrane, when IEC is reduced from 1.72 meq g<sup>-1</sup> to 1.58 meq g<sup>-1</sup> (almost 20%), the anion conductivity declined by 47%.<sup>86</sup>

It should be noted that the ion transport characteristic is also affected by chemical structures. This factor is correlated with the flexibility of polymer chains, which is also related to the types of ion exchange groups. The ion species can also contribute to the various ion sizes (radius), electronegativity, and hydration forces. The internal structure of membranes also influences their phase-separation and ion conductive channel formation.<sup>86</sup>

### 5.3. Providing structural durability

The structure of aligned nanofibers is promising to improve the mechanical integrity and structural stability of fuel cells. This structure supports the endurance to deformation and maintenance of structural integrity during fuel cell operation. An aligned nanofiber assembly is superior to a randomized one, considering that this structure maximizes the exposure of the catalyst surface area to the reactants. This structure facilitates a higher fraction of catalyst, enhancing the catalytic activity, leading to more efficient electrochemical reactions, and enhancing the fuel cell performance. A comparison between a conventional porous support and carbon nanofiber support is shown in Fig. 7. The aligned structure facilitates better adhesion and anchoring of the catalyst material, reducing its detachment or degradation during fuel cell operation, and

the improved durability contributes to a longer catalyst duration. Characteristics including mechanical properties and thermal stability can represent the structural durability of fuel cells.

Mechanical properties are crucial characteristics concerning the operational condition of fuel cells. The fuel cell membrane must endure the stress and withstand the mechanical degradation generated by physical and chemical stresses.<sup>87</sup> Mechanical properties are defined as the properties of materials in response to an applied load.<sup>20</sup> It has been reported that the essential mechanical properties to assess fuel cells include the modulus, tensile strength, and elongation at break. The modulus, also known as the elastic modulus, is the elasticity of a material.

Theoretically, by transforming isotropic nanofibers to more oriented nanofibers, for instance, in one axial direction, the mechanical properties of the nanofiber can be enhanced. It has been reported that the geometrical aspects can support the performance of fuel cells. In fuel cell application, this occurrence is also shown in proton exchange membrane application.<sup>18,63</sup> It has also been noted that with this approach, the modulus could increase up to 600% (from 1 MPa to > 7 MPa).<sup>62</sup> This observation was found in poly( $\epsilon$ -caprolactone) (PCL), which can be applied as a scaffold in tissue engineering. This experiment strengthened the evidence that changing the geometry of nanofibers to align can increase their mechanical properties. This observation opens a new opportunity to explore the effect of geometry on mechanical properties and other related functional fuel cell characteristics.

Thermal stability is also an important aspect of fuel cells because these devices operate within a certain temperature range, which refers to the stability of the sample when heat is applied. Thermogravimetric analysis (TGA) is a method that can be used to determine this characteristic. This method measures the weight change when a sample is heated.<sup>88</sup> It has been mentioned that the combination of TGA and FTIR is reliable for analyzing specific properties.<sup>89</sup> TGA is employed to investigate the changes in mass as a function of temperature and time. This test gives data regarding the analysis of thermal decomposition. Nonetheless, this method cannot identify the material during the heating experiment, and thus by combining it with FTIR, which provides the characteristic spectrum of the material, this analytical problem could be addressed.

It has been reported that uniaxial aligned nanofibers containing SPPEK-ZCCH exhibited good thermal stability.<sup>18</sup> The result showed that with aligned nanofibers, the stability was higher compared to the starting decomposition temperature of pure ZCCH. This happened because the frameworks of ZCCH are protected by SPPEK wrapped on its surface. It was also mentioned that aligned nanofibers could give a different result regarding thermal stability in proton exchange membrane and anion exchange membrane application. In a proton exchange membrane (sulfonated copolyimide nanofiber), according to the reported results, at 200 °C, the thermal stability was 90% compared to the ion exchange membrane (QAFPK-1-6-E nanofiber), which showed a value of 93%. However, when the temperature increased to 400 °C,<sup>90</sup> the

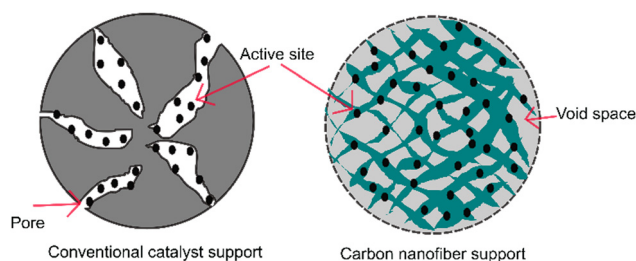


Fig. 7 Comparison of a conventional porous support (left) and carbon nanofiber support (right).



proton exchange membrane showed a value of 75%. Meanwhile, the anion exchange membrane presented a value of 70%.<sup>81</sup> In high-temperature proton exchange membrane fuel cells (HT-PEMFC), their operating temperatures were reported to be in the range of 120 °C and 200 °C.<sup>22</sup> In anion exchange membrane fuel cells (AEMFC), their operating temperature is usually in the range of 50 °C and 80 °C to avoid the degradation of the polymer.<sup>91</sup>

#### 5.4. Reduced water flooding

Aligned nanofibers show potential for competent water management, preventing water flooding during the fuel cell operation. When excessive liquid water accumulates in the electrode pores, water flooding occurs in fuel cells. This event blocks the reactant gases from accessing the catalyst sites. Aligned nanofibers are promising because their structure can act as capillary channels. Theoretically, aligned nanofibers have better characteristics because of their controlled orientation. This structure allows consistent and reproducible measurements during swelling tests, given that the dimensional changes can be precisely monitored along the aligned direction. Aligned nanofibers also promise to facilitate anisotropic swelling analysis. Fig. 8 illustrates the mechanism of nanofiber suppressing the swelling of the matrix.<sup>92,93</sup>

It has been mentioned that the swelling ratio and water uptake could decrease by using aligned nanofibers. The swelling test could be performed *via* two approaches, *i.e.*, swelling degree (SD) and water uptake (WU), which was carried out to determine the ratio of fibre expansion. The swelling degree and water uptake were investigated by soaking the samples in water. The swelling degree assesses the changes in sample volume caused by water absorption. The Flory Huggins equation is applied to measure the swelling degree and water uptake.<sup>94</sup>

In the proton exchange membrane application, the swelling of the aligned nanofibers based on SPESSK material decreased compared to the solution-casted membrane from 21% to 18%. In this experiment, the water uptake decreased from 36% to 34%.<sup>17</sup> In alkaline fuel cells, the result also showed a similar outcome. The quaternized-poly(arylene ether sulfone) (Q-PAES) aligned nanofiber exhibited decreased swelling properties. The water uptake was reduced from  $7.2\% \pm 0.4\%$  to  $2.8\% \pm 0.9\%$  according to the chloride anion ( $\text{Cl}^-$ ) measurement.<sup>80</sup>



Fig. 8 Mechanism of the nanofiber suppressing the swelling of the matrix.<sup>92,93</sup>

## 6. Opportunity: prospects and challenges

The prospects of aligned nanofiber can be seen in Fig. 9. It can be seen in Fig. 9(a), the journal article publications have a favourable profile in nanofiber application and aligned nanofiber structures. The gap in the number of publications indicates that there is significant opportunity to develop aligned nanofibers, and filling the gap can be one of the approaches to improve the previous research. Based on a heat map of the IPCR classification code, as presented in Fig. 9(b). The main invention of nanofibers in fuel cells is correlated with electrodes with catalytic activity, solid electrolytes, process of manufacture, platinum, and selection of catalytic material. The bibliometric study of this approach is shown in Fig. 9(c), indicating that there are three clusters of nanofiber and alignment. The vital keywords related to aligned nanofibers have co-occurrence, including nanofiber, alignment, performance, membrane, temperature, pore structure, and property.

Regarding fuel cell application, the aligned nanofiber enhances the PEMFC performance and can be further exploited in HT-PEMFC applications. In PEMFC, this structure is reported to lead to better proton conductivity, gas permeability, and stability considering chemical, thermal, and mechanical aspects.<sup>95</sup> Table 3 presents a summary of the current applications of aligned nanofibers, which are dominated by PEMFC. In the case of HT-PMFC, aligned nanofibers are strongly recommended due to their sustained lifespan and prevention of rapid degradation. Furthermore, implementing an aligned nanofiber structure can address the challenges of this type of fuel cell, such as heat management, heat resistance, and providing effective catalysts at high temperatures.

The challenge of developing aligned nanofibers despite their superior characteristics can be seen from industrialization and scientific engineering aspects. Regarding industrialization, the application of aligned nanofibers sometimes face the cost of manufacturing, considering that in some strategies, additional parts are necessary to fabricate aligned nanofibers, increasing the total cost of manufacturing. In the case of the second point of view, the type of material itself should also be mentioned because some materials act and have to be treated differently considering their unique characteristics; for instance, in a guide column array, a calcination process is conducted to produce aligned nanofibers with ceramic materials.<sup>13</sup> However, the uniqueness of materials also has advantages to mix their superior properties. The composition of nanofibers also affects the performance of fuel cells. Composite materials have the advantage of mixing the advantageous properties of each component material. For instance, in the case of a material that needs to be improved, for instance withstanding a higher mechanical load, a material that has good mechanical strength can be added to the composition. The preparation and characterization of polymer-based composite membranes for anion exchange membrane fuel cells using composite PVA-based materials have been reported. This polymer is promising to improve the performances of fuel cells due to the presence of



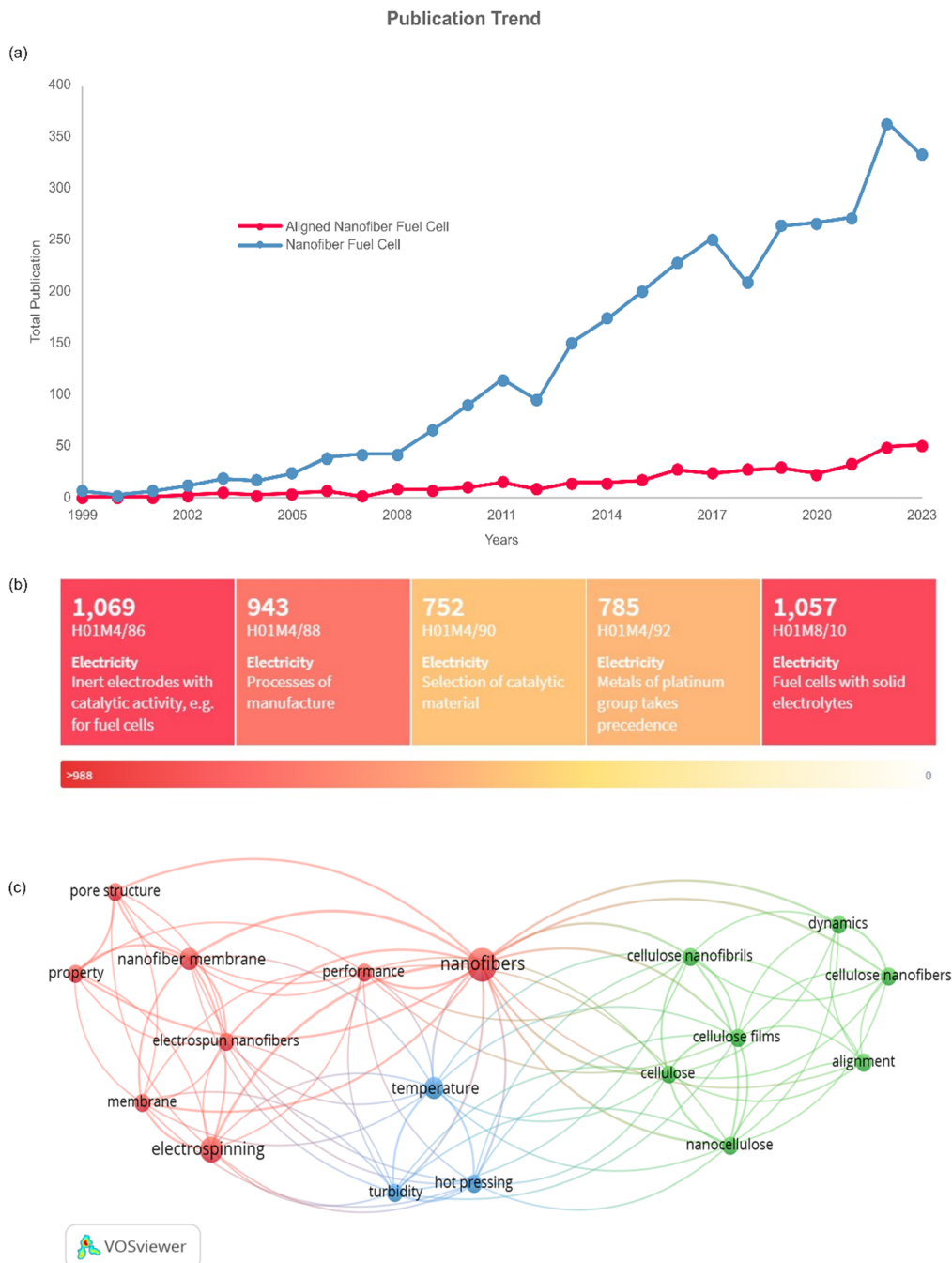


**Fig. 9** Trend of fuel cell research development: (a) comparison of total publications with the keywords “nanofiber” and “fuel cell” with “aligned”, “nanofiber”, and “fuel cell”, source: lens.org; (b) top 5 IPCR classification code sources, keywords: nanofiber AND fuel cell, source: lens.org and (c) bibliometric analysis by co-occurrence of keywords align AND nanofiber source: scopus.com, generated by VOSviewer. All data accessed on 07 April 2024.

reactive functional groups, which are valuable for improving the properties of the membrane by chemical crosslinking or other chemical modification.<sup>87,97</sup> A study aimed to achieve good OH<sup>−</sup> conductivity, high mechanical properties, and excellent chemical stability. The results showed that the composite could offer new prospects for alkaline polymer electrolyte fuel cells.

Finding the optimum value in some cases also must be considered because bigger is not always better correlated with

the characteristic fuel cell itself. For instance, it has been mentioned that the content of electrolyte in the active layer should be at an optimum value. When the substance content is too low, the problem is that not all the catalyst particles are connected to the electrolyte. When the substance content is too high, the gas diffusion is hindered, making the support material electrically isolated.<sup>98</sup> Optimization is necessary to find the optimum value for improving the fuel cell performance.

Table 3 Reported aligned nanofibers for application in fuel cells

| Result                                    |                        |                 |                           |               |                                    |                               |                                                   |                     |                           |                           |                                 |                  |                       |
|-------------------------------------------|------------------------|-----------------|---------------------------|---------------|------------------------------------|-------------------------------|---------------------------------------------------|---------------------|---------------------------|---------------------------|---------------------------------|------------------|-----------------------|
| Method/strategy                           | Material(s)            | Morphology (nm) | Mechanical strength (MPa) |               | Conductivity (S cm <sup>-1</sup> ) |                               | IEC (mmol g <sup>-1</sup> / meq g <sup>-1</sup> ) |                     | Swelling test (%)         |                           | Thermal stability (weight loss) |                  | Ref.                  |
|                                           |                        |                 | Non-aligned               | Aligned       | Non-aligned                        | Aligned                       | Non-aligned                                       | Aligned             | Non-aligned               | Aligned                   | Non-aligned                     | Aligned          |                       |
| Rotation speed (5000 rpm)                 | MOFs and SPPESEK       | 200             | $\sigma = 17.5$           | $\sigma = 27$ | $5.9 \times 10^{-2}$ (160 °C)      | $8.2 \times 10^{-2}$ (160 °C) | N/A                                               | N/A                 | N/A                       | N/A                       | $\pm 3\%$ (160)                 | $\pm 11\%$ (300) | PEMFC 18              |
| Rotation speed (> 1000 rpm)               | SPPESEK                | 157 ± 52        | $E = 15.8$                | $E = 19.3$    | $2.13 \times 10^{-2}$              | $3.66 \times 10^{-2}$ (50 °C) | 1.82                                              | 1.82                | SR = ±21                  | N/A                       | $\pm 4\%$ (300)                 | $\pm 16\%$ (400) | PEMFC 17              |
|                                           |                        |                 |                           |               |                                    |                               |                                                   |                     | WU = ± 36                 | WU = ± 34                 | $\pm 23\%$ (400)                | $\pm 2\%$ (160)  |                       |
| Two conductive strips                     | Sulfonated polyimide   | 199 ± 37        | N/A                       | N/A           | $3.6 \times 10^{-2}$ (80 °C)       | $8.8 \times 10^{-2}$ (80 °C)  | N/A                                               | N/A                 | *Casting Water uptake 22* | Water uptake 29           | N/A                             | N/A              | PEMFC 69              |
| Rotation speed (305 m min <sup>-1</sup> ) | SPEEK                  | 112–131         | N/A                       | N/A           | $7.22 \times 10^{-2}$              | $9.07 \times 10^{-2}$         | N/A                                               | N/A                 | *Without nanofiber        | N/A                       | N/A                             | N/A              | PEMFC 66              |
| Two conductive strips                     | Sulfonated copolyimide | 80–160          | N/A                       | N/A           | $8.36 \times 10^{-2}$ (90 °C)      | $12.2 \times 10^{-2}$ (90 °C) | 1.65                                              | 1.65                | Water uptake              | Water uptake              | $\pm 10\%$ (200)                | $\pm 10\%$ (200) | PEMFC 90              |
|                                           |                        |                 |                           |               | *Without nanofiber                 |                               |                                                   |                     | 32%                       | 42%                       | $\pm 25\%$ (400)                | $\pm 25\%$ (400) | PEMFC 96              |
|                                           |                        |                 |                           |               |                                    |                               |                                                   |                     | *Without nanofiber        |                           | $\pm 40\%$ (700)                | $\pm 55\%$ (700) |                       |
| Two conductive strips                     | Sulfonated polyimide   | 108 ± 22        | N/A                       | N/A           | $1 \times 10^{-4}$ (90 °C)         | $8.2 \times 10^{-2}$ (90 °C)  | N/A                                               | 1.65                | N/A                       | N/A                       | N/A                             | N/A              | PEMFC 96              |
| Two conductive strips                     | Q-PAES                 | 137 ± 23        | N/A                       | N/A           | $24 \times 10^{-2}$ (90 °C)        | $140 \times 10^{-2}$ (90 °C)  | N/A                                               | 1.72                | 7.2 ± 0.4                 | 2.8 ± 0.9 Cl <sup>-</sup> | N/A                             | N/A              | AFC, air batteries 80 |
| Rotation speed (2800 rpm)                 | QAAPPK-1-6-E           | 590± 180        | N/A                       | $\sigma = 54$ | $0.9 \times 10^{-2}$ (80 °C)       | $1.81 \times 10^{-2}$ (80 °C) | 2.14 ± 0.24 (80 °C)                               | 2.30 ± 0.18 (80 °C) | N/A                       | ±22% (80 °C)              | N/A                             | ±7% (200)        | AEMFC 81              |
|                                           |                        |                 |                           |               | OH <sup>-</sup>                    | OH <sup>-</sup>               | OH <sup>-</sup>                                   | OH <sup>-</sup>     |                           |                           |                                 | ±11% (300)       |                       |
|                                           |                        |                 |                           |               |                                    |                               |                                                   |                     |                           |                           |                                 | ±30% (400)       |                       |



**Table 4** The applications of nanofibers and their influence in fuel cells adapted from 103

| Application | Material                                                                                                                   | Type                         | Result/effect                                                                                                                                                  | Ref. |
|-------------|----------------------------------------------------------------------------------------------------------------------------|------------------------------|----------------------------------------------------------------------------------------------------------------------------------------------------------------|------|
| Cathode     | Hydrophobic graphitized carbon, PAN                                                                                        | PEFC                         | Decreasing water flooding                                                                                                                                      | 114  |
| Cathode     | Nafion/PVDF                                                                                                                | PEFC                         | Lowering carbon corrosion enhanced stress                                                                                                                      | 112  |
| Cathode     | Nafion/PAA, PtCo/C and Pt/C catalyst powders                                                                               | PEFC                         | Showing a better initial functioning as well as a superior long-term strength for the electrospun cathodes                                                     | 137  |
| Cathode     | PAA                                                                                                                        | PEFC                         | Decreasing agglomerations of platinum on carbon catalyst elements in catalyst inks                                                                             | 116  |
| Cathode     | PAA/Nafion                                                                                                                 | PEFC                         | Performing under low and high feed gas humidification                                                                                                          | 117  |
| Cathode     | Graphene fixed PAN/PVDF (GPP)                                                                                              | PEFC                         | Improving electrical conductivity and high porosity. Improving the triple reaction boundary. Stimulate gas and water transport throughout the porous electrode | 107  |
| Cathode     | SPEEK fixed with SCNFs                                                                                                     | DEFC                         | Increasing mechanical strength, proton conductivity, and reduced methanol permeability                                                                         | 111  |
| Cathode     | CNx sheet on PAN obliged by the Nafion distribution                                                                        | DEFC                         | Performing a power density resembling gold or platinum catalysts.                                                                                              | 138  |
| Cathode     | Carbon nitride/polyacrylonitrile nanofibers                                                                                | DEFC                         | Improving in oxygen reduction reaction activity                                                                                                                | 110  |
| Cathode     | PAN, Fe–N/C                                                                                                                | DEFC                         | Assisting active sites, assisted oxygen supply to the active surfaces                                                                                          | 115  |
| Cathode     | Lanthanum strontium cobalt ferrite (LSCF)                                                                                  | MCFC                         | Reducing operation temperature to (750 °C)                                                                                                                     | 139  |
| Cathode     | Ytria-stabilized zirconia with the penetrated LSM                                                                          | MCFC                         | Enhancing catalytic activity toward oxygen reduction                                                                                                           | 108  |
| Cathode     | LSCF                                                                                                                       | MCFC                         | Having low operation reduction at (750 °C)                                                                                                                     | 113  |
| Cathode     | (LSCF) tubes/(GDC) nanoparticles                                                                                           | MCFC                         | Having a reduce operational temperature (650 °C)                                                                                                               | 140  |
| Cathode     | Sm <sub>0.5</sub> Sr <sub>0.5</sub> CoO <sub>3-δ</sub> and Gd <sub>0.2</sub> Ce <sub>0.8</sub> O <sub>1.9</sub>            | MCFC                         | Performing major improve of the electrode working                                                                                                              | 141  |
| Cathode     | Polyacrylonitrile pyro polymer                                                                                             | PAFC                         | Improving polarization and improved catalytic activity                                                                                                         | 109  |
| Cathode     | Polyacrylonitrile                                                                                                          | PAFC                         | Being used as the gas diffusion electrodes in high temperature hydrogen                                                                                        | 142  |
| Cathode     | FeCo–CNF                                                                                                                   | AFC                          | Possessing the equivalent electrocatalytic activity. Higher tolerance to cross overed ethanol compared with Pt/C in the ORR                                    | 143  |
| Anode       | TiO <sub>2</sub> –C/C                                                                                                      | Microbial Fuel Cell (MFC)    | Having good electrical performance                                                                                                                             | 128  |
| Anode       | CNTs/CNF                                                                                                                   | MFC                          | Exhibiting a better conductivity, biocompatibility, hydrophilicity and electrocatalytic activity                                                               | 123  |
| Anode       | ACNF, with and without CNTs                                                                                                | MFC                          | Performing the high electrode conductivity, stability, and biocompatibility                                                                                    | 124  |
| Anode       | N–CNFs                                                                                                                     | MFC                          | Decreasing the process costs simultaneously while retaining excellent properties                                                                               | 125  |
| Anode       | ACNF                                                                                                                       | MFC                          | Reporting ACNF exhibited better performance than carbon anodes granular activated carbon, carbon cloth                                                         | 126  |
| Anode       | NiSn alloy nanoparticle, nickel acetate, tin chloride and PVA                                                              | Direct Urea Fuel Cell (DUFC) | Improving activity for oxidation, a high current density for urea oxidation                                                                                    | 118  |
| Anode       | PVA, Ni/Pd–C                                                                                                               | DUFC                         | Reporting urea concentration and polarized potential on the impedance behavior                                                                                 | 127  |
| Anode       | Ni/Cd-decorated electrospun carbon nanofibers                                                                              | DUFC                         | Reporting the low catalytic activity of the anode, extensively increased electrocatalytic activity for urea oxidation,                                         | 119  |
| Anode       | La <sub>x</sub> Sr <sub>1-x</sub> TiO <sub>3</sub> –Gd <sub>y</sub> Ce <sub>1-y</sub> O <sub>2-δ</sub>                     | SOFC                         | improve the electrochemical performance                                                                                                                        | 144  |
| Anode       | La <sub>0.4</sub> Sr <sub>0.6</sub> TiO <sub>3</sub> (LST), YSZ, Gd <sub>0.2</sub> Ce <sub>0.8</sub> O <sub>1.9</sub> , Ni | SOFC                         | Showing Decent thermal and redox cycling solidity                                                                                                              | 120  |
| Anode       | Ni-coated yttria-stabilized zirconia                                                                                       | SOFC                         | Enhancing the electrochemical reaction sites and also to reduce the difficulties for gas diffusion.                                                            | 121  |
| Anode       | SrCe <sub>0.8</sub> Y <sub>0.2</sub> O <sub>3-δ</sub> –Ni                                                                  | SOFC                         | Showing enhancement mechanism in calcined particle properties and proton hopping distance.                                                                     | 145  |
| Anode       | Sr <sub>2</sub> FeTiO <sub>6-δ</sub>                                                                                       | SOFC                         | Indicating that SFT is an actual promising electrode candidate (IT-SOFCs with SDC electrolyte)                                                                 | 146  |
| Anode       | Carbon–CeO <sub>2</sub>                                                                                                    | DMFC                         | Enhancing the electrochemical performance at concurrently lowered platinum loading                                                                             | 122  |
| Anode       | Carbon–CeO <sub>2</sub> , nickel acetate tetrahydrate, (PVA) and urea                                                      | DMFC                         | Proposing approach developed carbon nanofibers containing nickel nanoparticles and fixed by nitrogen.                                                          | 147  |
| Anode       | PVDF/Pt–Pd/RGO–CeO <sub>2</sub>                                                                                            | DMFC                         | PVDF–Pt–Pd/RGO–CeO <sub>2</sub> as the new catalyst material for DMFC.                                                                                         | 148  |
| Anode       | TiO <sub>2</sub> carbon                                                                                                    | DMFC                         | Ensuring that the best catalytic material focuses on the fabrication of a new composite TiO <sub>2</sub> carbon nanofiber anodic catalyst support              | 129  |
| Anode       | Polyacrylonitrile (PAN), A TiO <sub>2</sub> -embedded carbon nanofiber (TECNF)                                             | DMFC                         | TECNF is a promising support of the PtRu nanocatalyst for the methanol oxidation reaction                                                                      | 149  |
| Anode       | Polypyrrole nanowire networks (PPNNs)                                                                                      | DMFC                         | Showing significantly improves catalyst utilization and mass transfer of methanol on the anode.                                                                | 150  |



Table 4 (continued)

| Application | Material                                                                                                                                        | Type                                           | Result/effect                                                                                                                                                    | Ref. |
|-------------|-------------------------------------------------------------------------------------------------------------------------------------------------|------------------------------------------------|------------------------------------------------------------------------------------------------------------------------------------------------------------------|------|
| Anode       | CeO <sub>2</sub> -C with Pt-Co nanoparticles                                                                                                    | DMFC                                           | Proposing the combination of two effective systems, <i>i.e.</i> CeO <sub>2</sub> -C and Pt-Co                                                                    | 151  |
| Membrane    | Nafion perfluorosulfonic acid/PVDF                                                                                                              | SOFC                                           | Providing a fabrication strategy for high-performance electrodes                                                                                                 | 132  |
| Membrane    | Nafion <sup>®</sup> PFSA and PVDF                                                                                                               | H <sub>2</sub> Br <sub>2</sub> fuel cells      | Increasing PVDF content declines in proton conductivity, water/electrolyte swelling and permeability                                                             | 152  |
| Membrane    | Nafion/polyphenylsulfone                                                                                                                        | PEFC                                           | Showing excellent water swelling and mechanical properties as well as proton conductivity                                                                        | 153  |
| Membrane    | Nafion <sup>®</sup> perfluorosulfonic acid (PFSA) ionomer for proton transport and polyvinylidene fluoride (PVDF) for mechanical reinforcement. | Hydrogen/bromine fuel cell                     | Fabricating and characterizing nanofiber composite for regenerative hydrogen/bromine fuel cell                                                                   | 154  |
| Membrane    | Nafion <sup>®</sup> PFSA, polyphenylsulfone (PPSU)                                                                                              | H <sub>2</sub> /Br <sub>2</sub> -HBr fuel cell | Reporting nanofiber composite membranes can overcome the high cost of PFSA                                                                                       | 155  |
| Membrane    | Polyvinylidene fluoride (PVDF)/Nafion                                                                                                           | MFC                                            | Producing electricity from a single culture MFC                                                                                                                  | 135  |
| Membrane    | SPPESEK                                                                                                                                         | PEFC                                           | Enhancements on open circuit voltage and power density. Fiberization increases proton conductivity, swelling resistance, and mechanical and thermal stabilities. | 130  |
| Membrane    | PVDF/Nafion                                                                                                                                     | PEFC                                           | Obtaining <i>via</i> electrospinning experiencing a “reciprocal templating” experience that performs electrical performance                                      | 156  |
| Membrane    | SPPESEK and poly(phenylene oxide)                                                                                                               | Bipolar membrane (BPM)                         | Performing electrodialysis, hydrogen production, and self-humidifying fuel cells                                                                                 | 131  |
| Membrane    | MOFs and SPPESEK                                                                                                                                | PEFC                                           | Increase proton conductivity (aligned nanofiber)                                                                                                                 | 18   |
| Membrane    | SPPESEK                                                                                                                                         | DMFC                                           | Increasing conductivity in the thickness aligned. Enhancing single cell power density and tensile strength                                                       | 17   |
| Membrane    | Sulfonated polyimide                                                                                                                            | PEFC                                           | Performing the membrane stability, Decreasing oxygen permeability                                                                                                | 157  |

Nanofibers are well known for their significant applications in a wide range of electrochemical devices. It has been reported that this technology is implemented in batteries, sensors, supercapacitors, photovoltaic cells, electrolysis, and fuel cells. Nanofibers are used as electrolytes, cathode materials, anode materials, and separators in batteries.

Electrospinning results in a high surface-to-volume ratio. This characteristic can be used in several electrolytic cell purposes, for instance, dye-degradation applications,<sup>99</sup> water dissociation or splitting,<sup>100</sup> and disinfection of water (from urea, for example).<sup>101</sup> In sensor application, the fibre structure and orientation were reported to lead to high sensitivity.<sup>102</sup> In electrochemical solar cell application, dye-sensitized solar cells (DSSCs) or perovskite solar cells can be explored using this approach.<sup>103</sup> The application of nanofibers in batteries can improve their cyclic stability<sup>104</sup> and enhance their capacity.<sup>105</sup> The highly porous structure has the advantage of reducing the degradation rate during charging or discharging.<sup>105</sup> Coating methods can also improve their structure, which leads to faster diffusion.<sup>103</sup> According to the operating mechanism of the supercapacitor, its performance is affected by surface area and morphology. Numerous studies have illustrated that an optimized pore size and surface area can improve the performance of electrodes. It has been reported that carbon-based nanofibrous materials can improve the ion migration to the active surfaces, leading to enhanced interfacial charge transportation.<sup>103,106</sup>

Nanofibers have been widely used in fuel cell research due to their advantages, resulting in promising characteristics. In fuel

cell application, nanofibers can be used as mats that could be implemented as a membrane, cathode material or anode material. The advantage of the electrospinning manufacturing process is its capability to tailor the morphology, leading to enhanced physical and chemical material properties.

Nanofibers are implemented to improve the cathode function and are successfully constructed in fuel cell applications. Regarding ion transfer properties, the results showed that the advantages of adding these structures are improving the electrical conductivity<sup>107</sup> and enhancing the catalytic activity toward oxygen reduction.<sup>108–110</sup> Concerning mechanical properties, these structures successfully increased the mechanical strength<sup>111</sup> and lowered carbon corrosion.<sup>112</sup> Another interesting observation was that by adding nanofibers or transforming structures into nanofibers, the temperature operation could be lower<sup>108,113</sup> and the water flooding also decreased.<sup>114</sup> The popular materials for building cathodes are composite-based materials using PAN,<sup>107,114,115</sup> PVDF,<sup>107,112</sup> and PAA.<sup>116,117</sup>

The anode can also be improved by adding nanofibers. Benefits such as improving activity for oxidation,<sup>118,119</sup> showing decent thermal and redox cycling stability,<sup>120</sup> reducing the barriers for gas diffusion,<sup>121</sup> and enhancing the electrochemical performance at a concurrently lowered platinum<sup>122</sup> loading are noted due to the application of nanofiber assemblies. The structured materials utilized to fabricate nanofiber structures for the anode in fuel cells include carbon nanotubes (CNT),<sup>120</sup> carbon nanofibers (CNF),<sup>123–126</sup> nickel/cadmium,<sup>121,127</sup> PVA,<sup>118,127</sup> and TiO<sub>2</sub>.<sup>128,129</sup>

Regarding the membrane, its main characteristics are also enhanced by adding nanofiber structures. Specific properties



such as conductivity, mechanical integrity, and chemical stability also result in better performances. It has been reported that materials such as SPPEK<sup>17,18,130,131</sup> and PVDF<sup>132–136</sup> can be highly engineered to create a better membrane. Interestingly, the anion exchange membrane has not been highly explored to date compared to the proton exchange membrane. This finding opens the opportunity to seek aligned nanofibers to improve the performance in this type of fuel cell, considering that this type of fuel cell has advantages, especially in terms of reduced cost and high efficiency. Table 4 shows the reports on nanofiber application in fuel cells in detail, and their results are highlighted.

## 7. Conclusion

Herein, the use of aligned nanofiber structures was elaborated as a promising strategy to improve the performance of fuel cells. This type of structure can be fabricated in a versatile way using the electrospinning method. To date, although various fabrication techniques have been developed utilizing this apparatus, the simplest way to achieve an aligned structure is by increasing the speed of the rotating drum collector (800–5000 rpm). An exciting approach is modifying the patterned strip (two, four, or six strips) on the collector as an electrode. The results showed that this technique produced one, two, and three axial lines, respectively.

Concerning why aligned nanofiber can improve the fuel cell performance, the effect of aligned nanofibers on conductivity was explained. This structure network provides a proton channel structure, enhancing the rapid transport of protons. As a result, an excellent through-plane proton transport performance was shown in the fuel cell operation. It was also reported that the anionic conductivity could be increased by 10–15 times. Regarding mass transport, it should be noted that the ion transport characteristic is also affected by chemical structures. This factor is correlated with the flexibility of the polymer chains and related to the types of ion exchange groups. The most remarkable result is that oriented nanofibers provided structural durability. The mechanical strength was reported to be enhanced by up to 600%, which is an essential property in fuel cells under highly dynamic operating conditions. Aligned nanofibers also promise to reduce the weight loss due to the fuel cell operation. It has been mentioned that the frameworks of certain materials can be protected by nanofibers wrapped on their surface. To reduce water flooding, it has been mentioned that the swelling ratio and water uptake can decrease by using aligned nanofibers. This result is promising for a practical fuel cell operation, considering that an ideal component, such as a membrane, should have highly depressed water absorption.

All the above-mentioned results open new opportunities for research into this promising approach, which improves the performance of fuel cells through the geometry and alignment of nanofibers. The advantage of the electrospinning manufacturing process is that the capability to tailor the morphology leads to enhanced physical and chemical material properties.

The complexity and additional manufacturing should also be considered and the characteristics of the material and optimum condition need to be determined as challenges in this approach. Nevertheless, the potential of using aligned nanofiber structures and the key influencing parameters for the development of fuel cells still need to be extensively investigated. Research into future applications of this technology is still in its infancy, but in fuel cells alone, it can be used as the membrane, anode, and cathode materials.

## Author contributions

Conceptualization, M. Y. and V. H.; writing – original draft, M. Y.; writing – review and editing, M. Y. and V. H.; visualization, M. Y.; supervision, V. H.; funding acquisition, V. H. All authors have read and agreed to the published version of the manuscript.

## Conflicts of interest

There are no conflicts to declare.

## Acknowledgements

The authors would like to thank the Open Access Funding by TU Graz Open Access Publishing Fund. Additionally, the authors acknowledge the IEA Research Co-operation on behalf of the Austrian Federal Ministry for Climate Action, Environment, Energy, Mobility, Innovation and Technology, and OeAD (Austria) for the Ernst Mach Grant ASEA-UNINET scholarship.

## Notes and references

- 1 C. Zou, Q. Zhao, G. Zhang and B. Xiong, Energy revolution: from a fossil energy era to a new energy era, *Nat. Gas Ind. B*, 2016, **3**, 1–11.
- 2 C. Schelly, D. Bessette, K. Brosemer, V. Gagnon, K. L. Arola, A. Fiss, J. M. Pearce and K. E. Halvorsen, Energy policy for energy sovereignty: can policy tools enhance energy sovereignty?, *Sol. Energy*, 2020, **205**, 109–112.
- 3 H. Chen, T. N. Cong, W. Yang, C. Tan, Y. Li and Y. Ding, Progress in electrical energy storage system: a critical review, *Prog. Nat. Sci.*, 2009, **19**, 291–312.
- 4 I. S. Chronakis, Novel nanocomposites and nanoceramics based on polymer nanofibers using electrospinning process – A review, *J. Mater. Process. Technol.*, 2005, **167**, 283–293.
- 5 X. Gong, G. He, X. Yan, Y. Wu, W. Chen and X. Wu, Electrospun nanofiber enhanced imidazolium-functionalized polysulfone composite anion exchange membranes, *RSC Adv.*, 2015, **5**, 95118–95125.
- 6 S. G. Peera, R. Koutavarapu, S. Akula, A. Asokan, P. Moni, M. Selvaraj, J. Balamurugan, S. O. Kim, C. Liu and A. K. Sahu, Carbon Nanofibers as Potential Catalyst Support for



- Fuel Cell Cathodes: A Review, *Energy Fuels*, 2021, **35**, 11761–11799.
- 7 C. Klose, M. Breitwieser, S. Vierrath, M. Klingele, H. Cho, A. Büchler, J. Kerres and S. Thiele, Electrospun sulfonated poly(ether ketone) nanofibers as proton conductive reinforcement for durable Nafion composite membranes, *J. Power Sources*, 2017, **361**, 237–242.
  - 8 J. Doshi and D. H. Reneker, Electrospinning process and applications of electrospun fibers, *Conf. Rec. - IAS Annu. Meet. (IEEE Ind. Appl. Soc.)*, 1993, **3**, 1698–1703.
  - 9 A. Theron, E. Zussman and A. Yarin, Electrostatic field-assisted alignment of electrospun nanofibre, *Nanotechnology*, 2001, **12**, 384–390.
  - 10 J. M. Deitzel, J. D. Kleinmeyer, J. K. Hirvonen and N. C. Beck Tan, Controlled deposition of electrospun poly(ethylene oxide) fibers, *Polymer*, 2001, **42**, 8163–8170.
  - 11 D. Li, Y. Ru, Z. Chen, C. Dong, Y. Dong and J. Liu, Accelerating the design and development of polymeric materials via deep learning: current status and future challenges, *APL Mach. Learn.*, 2023, **1**, 021501.
  - 12 F. Dabirian, S. Sarkeshik and A. Kianiha, Production of Uniaxially Aligned Nanofibers Using a Modified Electrospinning Method: Rotating Jet, *Curr. Nanosci.*, 2009, **5**, 318–323.
  - 13 M. A. K. Budi, A. Kubart and J. S. Andrew, Guide column array: a versatile approach to aligning and patterning ceramic nanofibers, *Nanoscale*, 2018, **10**, 20681–20688.
  - 14 J. Lee and Y. Deng, Increased mechanical properties of aligned and isotropic electrospun PVA nanofiber webs by cellulose nanowhisker reinforcement, *Macromol. Res.*, 2012, **20**, 76–83.
  - 15 G. Liu, F. Ye, L. Xiong, J. Lee, L. Wang, X. Li, J. Li, J. K. Lee and W. Yang, Cathode catalyst layer with nanofiber microstructure for direct methanol fuel cells, *Energy Convers. Manage.*, 2020, **218**, 113013.
  - 16 J. K. Chinthaginjala, K. Seshan and L. Lefferts, Preparation and application of carbon-nanofiber based microstructured materials as catalyst supports, *Ind. Eng. Chem. Res.*, 2007, **46**, 3968–3978.
  - 17 X. Gong, G. He, Y. Wu, S. Zhang, B. Chen, Y. Dai and X. Wu, Aligned electrospun nanofibers as proton conductive channels through thickness of sulfonated poly(phthalazinone ether sulfone ketone) proton exchange membranes, *J. Power Sources*, 2017, **358**, 134–141.
  - 18 B. Wu, J. Pan, L. Ge, L. Wu, H. Wang and T. Xu, Oriented MOF-polymer composite nanofiber membranes for high proton conductivity at high temperature and anhydrous condition, *Sci. Rep.*, 2014, **4**, 1–7.
  - 19 Y. Wang, K. S. Chen, J. Mishler, S. C. Cho and X. C. Adroher, A review of polymer electrolyte membrane fuel cells: technology, applications, and needs on fundamental research, *Appl. Energy*, 2011, **88**, 981–1007.
  - 20 A. M. Samsudin, M. Bodner and V. Hacker, A Brief Review of Poly(Vinyl Alcohol)-Based Anion Exchange Membranes for Alkaline Fuel Cells, *Polymers*, 2022, **14**, 1–26.
  - 21 EG&G Technical Services, Inc., *Fuel Cell Handbook*, U.S. Department of Energy Office of Fossil Energy National Energy Technology Laboratory, Morgantown, West Virginia, 7th edn, 2004.
  - 22 M. Cassir, D. Jones, A. Ringuedé and V. Lair, *Electrochemical devices for energy: Fuel cells and electrolytic cells*, 2013, **2**.
  - 23 R. E. Rosli, A. B. Sulong, W. R. W. Daud, M. A. Zulkifley, T. Husaini, M. I. Rosli, E. H. Majlan and M. A. Haque, A review of high-temperature proton exchange membrane fuel cell (HT-PEMFC) system, *Int. J. Hydrogen Energy*, 2017, **42**, 9293–9314.
  - 24 R. G. Bodkhe, R. L. Shrivastava, V. K. Soni and R. B. Chadge, A review of renewable hydrogen generation and proton exchange membrane fuel cell technology for sustainable energy development, *Int. J. Electrochem. Sci.*, 2023, **18**, 100108.
  - 25 M. Irvaninia and S. Rowshanzamir, Polysulfone-based Anion Exchange Membranes for Potential Application in Solid Alkaline Fuel Cells, *J. Renewable Energy Environ.*, 2015, **2**, 59–65.
  - 26 K. Kargupta, S. Saha, D. Banerjee, M. Seal and S. Ganguly, Performance enhancement of phosphoric acid fuel cell using phosphosilicate gel based electrolyte, *Ranlia Huaxue Xuebao*, 2012, **40**, 707–713.
  - 27 Fuel Cell & Hydrogen Energy Association, Phosphoric Acid Fuel Cell, <https://www.fchea.org/fc-types/911r9u6rfbm891j33hxjod7el0028>.
  - 28 E. Antolini, The stability of molten carbonate fuel cell electrodes: A review of recent improvements, *Appl. Energy*, 2011, **88**, 4274–4293.
  - 29 M. A. R. S. Al-Baghdadi, *Sch. Community Encycl.*, 2022.
  - 30 M. A. R. S. Al-Baghdadi, Computational Modeling Aspects of Polymer Electrolyte Fuel Cell Durability, *Computational Fluid Dynamics: Theory, Analysis and Applications*, Nova Science Publishers, Inc, New York USA, 2011, pp. 1–40.
  - 31 M. A. R. S. Al-Baghdadi and H. A. K. S. Al-Janabi, Influence of the design parameters in a proton exchange membrane (PEM) fuel cell on the mechanical behavior of the polymer membrane, *Energy Fuels*, 2007, **21**, 2258–2267.
  - 32 M. A. R. S. Al-Baghdadi, Proton exchange membrane fuel cells modeling: a review of the last ten years results of the Fuel Cell Research Center-IEEF, *Int. J. Energy Environ.*, 2017, **8**, 1–28.
  - 33 M. A. R. S. Al-Baghdadi and H. A. K. S. Al-Janabi, Effect of PEM fuel cell operation on gas diffusion layers and membrane stresses, *Int. J. Fluid Mech. Res.*, 2008, **35**, 219–234.
  - 34 M. A. R. S. Al-Baghdadi and H. A. K. S. Al-Janabi, Prediction of hygro-thermal stress distribution in proton exchange membranes using a three-dimensional multi-phase computational fluid dynamics model, *Proc. Inst. Mech. Eng., Part A*, 2007, **221**, 941–953.
  - 35 M. Yusro and R. Martien, Investigating Fluid Parameters in Nanofiber Biomaterial Fabrication using Electrospinning, *J. Energy, Mech. Mater. Manuf. Eng.*, 2020, **5**, 11–24.
  - 36 B. Swankaert, J. Geltmeyer, K. Rabaey, K. De Buysser, L. Bonin and K. De Clerck, A review on ion-exchange nanofiber membranes: properties, structure and application in





- electrochemical (waste)water treatment, *Sep. Purif. Technol.*, 2022, **287**, 1–45.
- 37 S. Imaizumi, H. Matsumoto, M. Ashizawa, M. Minagawa and A. Tanioka, Nanosize effects of sulfonated carbon nanofiber fabrics for high capacity ion-exchanger, *RSC Adv.*, 2012, **2**, 3109–3114.
  - 38 H. V. Mhetre, K. Y. Krishnarao and N. Naik, Optimization of electrospinning process parameters to develop the smallest ZnO + PVP nanofibres using Taguchi experimental design and ANOVA, *J. Mater. Sci.: Mater. Electron.*, 2023, **34**, 1–15.
  - 39 N. Amini, M. Kalaei, S. Mazinani, S. Pilevar and S. O. Ranaei-Siadat, Morphological optimization of electrospun polyacrylamide/MWCNTs nanocomposite nanofibers using Taguchi's experimental design, *Int. J. Adv. Manuf. Technol.*, 2013, **69**, 139–146.
  - 40 F. S. Alfares, E. Guler, H. Alenezi, M. E. Cam and M. Edirisinghe, Optimization of Process-Control Parameters for the Diameter of Electrospun Hydrophilic Polymeric Composite Nanofibers, *Macromol. Mater. Eng.*, 2021, **306**(12), 2100471.
  - 41 M. Elkasaby, H. A. Hegab, A. Mohany and G. M. Rizvi, Modeling and optimization of electrospinning of polyvinyl alcohol (PVA), *Adv. Polym. Technol.*, 2018, **37**, 2114–2122.
  - 42 H. Albetran, Y. Dong and I. M. Low, Characterization and optimization of electrospun TiO<sub>2</sub>/PVP nanofibers using Taguchi design of experiment method, *J. Asian Ceram. Soc.*, 2015, **3**, 292–300.
  - 43 Z. Zhou, X. F. Wu, X. Gao, L. Jiang, Y. Zhao and H. Fong, Parameter dependence of conic angle of nanofibres during electrospinning, *J. Phys. D: Appl. Phys.*, 2011, **44**(43), 435401.
  - 44 S. Suresh, A. Becker and B. Glasmacher, Impact of apparatus orientation and gravity in electrospinning—a review of empirical evidence, *Polymers*, 2020, **12**, 1–15.
  - 45 C. Akduman and E. P. A. Kumbasar, Electrospun Polyurethane Nanofibers, *Aspects Polyurethanes*, 2017 (September), 17–52, DOI: [10.5772/intechopen.69937](https://doi.org/10.5772/intechopen.69937).
  - 46 J. A. Abbas, I. A. Said, M. A. Mohamed, S. A. Yasin, Z. A. Ali and I. H. Ahmed, Electrospinning of polyethylene terephthalate (PET) nanofibers: optimization study using taguchi design of experiment, *IOP Conf. Ser. Mater. Sci. Eng.*, 2018, **454**, 012130.
  - 47 J. I. Kim, T. I. Hwang, L. E. Aguilar, C. H. Park and C. S. Kim, A Controlled Design of Aligned and Random Nanofibers for 3D Bi-functionalized Nerve Conduits Fabricated via a Novel Electrospinning Set-up, *Sci. Rep.*, 2016, **6**, 1–12.
  - 48 C. Ayres, G. L. Bowlin, S. C. Henderson, L. Taylor, J. Shultz, J. Alexander, T. A. Telemeco and D. G. Simpson, Modulation of anisotropy in electrospun tissue-engineering scaffolds: analysis of fiber alignment by the fast Fourier transform, *Biomaterials*, 2006, **27**, 5524–5534.
  - 49 N. E. Zander, Hierarchically structured electrospun fibers, *Polymers*, 2013, **5**, 19–44.
  - 50 H. Mohammad Khanlou, B. Chin Ang, S. Talebian, A. Muhammad Afifi and A. Andriyana, Electrospinning of polymethyl methacrylate nanofibers: optimization of processing parameters using the Taguchi design of experiments, *Text. Res. J.*, 2015, **85**, 356–368.
  - 51 A. Nazir, N. Khenoussi, L. Schacher, T. Hussain, D. Adolphe and A. H. Hekmati, Using the Taguchi method to investigate the effect of different parameters on mean diameter and variation in PA-6 nanofibres produced by needleless electrospinning, *RSC Adv.*, 2015, **5**, 76892–76897.
  - 52 M. Yusro, Assessing Beads Generation in Fabricating Nanofiber Bioactive Material-Based Associated with Its Fluid Factors, *Lect. Notes Electron. Eng.*, 2021, **746 LNEE**, 173–182.
  - 53 O. Hardick, B. Stevens and D. G. Bracewell, Nanofibre fabrication in a temperature and humidity controlled environment for improved fibre consistency, *J. Mater. Sci.*, 2011, **46**, 3890–3898.
  - 54 N. Bhardwaj and S. C. Kundu, Electrospinning: a fascinating fiber fabrication technique, *Biotechnol. Adv.*, 2010, **28**, 325–347.
  - 55 A. Haider, S. Haider and I.-K. Kang, A comprehensive review summarizing the effect of electrospinning parameters and potential applications of nanofibers in biomedical and biotechnology, *Arab. J. Chem.*, 2018, **11**, 1165–1188.
  - 56 S. De Vrieze, T. Van Camp, A. Nelvig, B. Hagström, P. Westbroek and K. De Clerck, The effect of temperature and humidity on electrospinning, *J. Mater. Sci.*, 2009, **44**, 1357–1362.
  - 57 D. Li, Y. Wang and Y. Xia, Electrospinning Nanofibers as Uniaxially Aligned Arrays and Layer-by-Layer Stacked Films, *Adv. Mater.*, 2004, **16**, 361–366.
  - 58 P. Katta, M. Alessandro, R. D. Ramsier and G. G. Chase, Continuous electrospinning of aligned polymer nanofibers onto a wire drum collector, *Nano Lett.*, 2004, **4**, 2215–2218.
  - 59 R. Dersch, T. Liu, A. K. Schaper, A. Greiner and J. H. Wendorff, Electrospun nanofibers: internal structure and intrinsic orientation, *J. Polym. Sci., Part A: Polym. Chem.*, 2003, **41**, 545–553.
  - 60 M. Khamfroush and M. Mahjob, Modification of the rotating jet method to generate highly aligned electrospun nanofibers, *Mater. Lett.*, 2011, **65**, 453–455.
  - 61 P. Nitti, N. Gallo, L. Natta, F. Scalera, B. Palazzo, A. Sannino and F. Gervaso, Influence of nanofiber orientation on morphological and mechanical properties of electrospun chitosan mats, *J. Healthcare Eng.*, 2018, **2018**, 3651480.
  - 62 B. M. Baker and R. L. Mauck, The Effect of Nanofiber Alignment on the Maturation of Engineered Meniscus Constructs, *Biomaterials*, 2007, **28**, 1967–1977.
  - 63 H. M. Paulya, D. J. Kelly, K. C. Popata, N. A. Trujillof, N. J. Dunneg, H. O. McCarthyi and T. L. H. Donahuea, Mechanical Properties and Cellular Response of Novel Electrospun Nanofibers for Ligament Tissue Engineering: Effects of Orientation and Geometry, *J. Mech. Behav. Biomed. Mater.*, 2016, **61**, 1–40.





- 64 L. Li, Y. Liu and Y. F. Li, Electrochemical degradation of methylene blue aqueous solution on electrospinning nanofibers (ESF) electrodes, *Adv. Mater. Res.*, 2013, **807–809**, 1362–1367.
- 65 S. D. Liu, D. Sen Li, Y. Yang and L. Jiang, Fabrication, mechanical properties and failure mechanism of random and aligned nanofiber membrane with different parameters, *Nanotechnol. Rev.*, 2019, **8**, 218–226.
- 66 M. J. Mehdi Sadrjehani, A. Akbar Gharehaghaji and M. Javanbakht, Aligned Electrospun Sulfonated Poly(ether ether ketone) Nanofiber-Based Proton Exchange Membranes for Fuel Cell Applications, *Polym. Eng. Sci.*, 2017, 789–796.
- 67 C. Y. Huang, K. H. Hu and Z. H. Wei, Comparison of cell behavior on pva/pva-gelatin electrospun nanofibers with random and aligned configuration, *Sci. Rep.*, 2016, **6**, 1–8.
- 68 D. Li, Y. Wang and Y. Xia, Electrospinning of polymeric and ceramic nanofibers as uniaxially aligned arrays, *Nano Lett.*, 2003, **3**, 1167–1171.
- 69 T. Tamura and H. Kawakami, Aligned electrospun nanofiber composite membranes for fuel cell electrolytes, *Nano Lett.*, 2010, **10**, 1324–1328.
- 70 S. H. Park and D.-Y. Yang, Fabrication of Aligned Electrospun Nanofibers by Inclined Gap Method, *J. Appl. Polym. Sci.*, 2011, **120**, 1800–1807.
- 71 T. A. Kowalewski and S. Barral, Modelling electrospinning of nanofibres, *PAMM*, 2009, **9**, 463–464.
- 72 O. Karatay and M. Dogan, Modelling of electrospinning process at various electric fields, *Micro Nano Lett.*, 2011, **6**, 858–862.
- 73 N. A. Norzain and W. C. Lin, Orientated and diameter-controlled fibrous scaffolds fabricated using the centrifugal electrospinning technique for stimulating the behaviours of fibroblast cells, *J. Ind. Text.*, 2022, **51**, 6728S–6752S.
- 74 Z. Zhang and J. Sun, Research on the development of the centrifugal spinning, *MATEC Web Conf.*, 2017, **95**, 07003.
- 75 G. Anusiya and R. Jaiganesh, A review on fabrication methods of nanofibers and a special focus on application of cellulose nanofibers, *Carbohydr. Polym. Technol. Appl.*, 2022, **4**, 41–55.
- 76 S. M. Taghavi and R. G. Larson, Regularized thin-fiber model for nanofiber formation by centrifugal spinning, *Phys. Rev. E: Stat., Nonlinear, Soft Matter Phys.*, 2014, **89**, 1–9.
- 77 S. Padron, A. Fuentes, D. Caruntu and K. Lozano, Experimental study of nanofiber production through forcespinning, *J. Appl. Phys.*, 2013, **113**(2), 024318.
- 78 L. Wu, Z. Zhang, J. Ran, D. Zhou, C. Li and T. Xu, Advances in proton-exchange membranes for fuel cells: an overview on proton conductive channels (PCCs), *Phys. Chem. Chem. Phys.*, 2013, **15**, 4870–4887.
- 79 M. B. DeGostin, A. A. Peracchio, T. D. Myles, B. N. Cassenti and W. K. S. Chiu, Charge transport in the electrospun nanofiber composite membrane's three-dimensional fibrous structure, *J. Power Sources*, 2016, **307**, 538–551.
- 80 T. Watanabe, M. Tanaka and H. Kawakami, Fabrication and electrolyte characterization of uniaxially-aligned anion conductive polymer nanofibers, *Nanoscale*, 2016, **8**, 19614–19619.
- 81 Y. C. Zhou, R. Y. Bao, Z. Liu, M. B. Yang and W. Yang, Electrospun Modified Polyketone-Based Anion Exchange Membranes with High Ionic Conductivity and Robust Mechanical Properties, *ACS Appl. Energy Mater.*, 2021, **4**, 5187–5200.
- 82 K. Bunzl and B. Sansoni, Determination of the ion exchange capacity of solid ion exchangers by difference weighting, *Anal. Chem.*, 1976, **48**, 2279–2280.
- 83 P. Kumar, R. P. Bharti, V. Kumar and P. P. Kundu, in *Progress and Recent Trends in Microbial Fuel Cells*, ed. P. P. Kundu and K. Dutta, Elsevier, 2018, pp. 47–72.
- 84 K. S. Spiegler, Transport processes in ionic membranes, *Trans. Faraday Soc.*, 1958, **54**, 1408–1428.
- 85 J. R. Varcoe, P. Atanassov, D. R. Dekel, A. M. Herring, M. A. Hickner, P. A. Kohl, A. R. Kucernak, W. E. Mustain, K. Nijmeijer, K. Scott, T. Xu and L. Zhuang, Anion-exchange membranes in electrochemical energy systems, *Energy Environ. Sci.*, 2014, **7**, 3135–3191.
- 86 T. Watanabe, M. Tanaka and H. Kawakami, Fabrication and electrolyte characterization of uniaxially-aligned anion conductive polymer nanofibers, *Nanoscale*, 2016, **8**, 19614–19619.
- 87 A. M. Samsudin, M. Roschger, S. Wolf and V. Hacker, Preparation and Characterization of QPVA/PDDA Electrospun Nanofiber Anion Exchange Membranes for Alkaline Fuel Cells, *Nanomaterials*, 2022, **12**(22), 3965.
- 88 S. Ebnessajjad, in *Handbook of Adhesives and Surface Preparation Technology, Applications and Manufacturing*, ed. S. Ebnessajjad, William Andrew Publishing, Norwich, NY, 2011, pp. 31–48.
- 89 J. Abraham, A. P. Mohammed, M. P. Ajith Kumar, S. C. George and S. Thomas, in *Micro and Nano Technologies*, ed. S. Mohan Bhagyaraj, O. S. Oluwafemi, N. Kalarikkal and S. B. T.-C. of N. Thomas, Woodhead Publishing, 2018, pp. 213–236.
- 90 T. Tamura, R. Takemori and H. Kawakami, Proton conductive properties of composite membranes containing uniaxially aligned ultrafine electrospun polyimide nanofiber, *J. Power Sources*, 2012, **217**, 135–141.
- 91 K. Yassin, I. G. Rasin, S. Willdorf-Cohen, C. E. Diesendruck, S. Brandon and D. R. Dekel, A surprising relation between operating temperature and stability of anion exchange membrane fuel cells, *J. Power Sources Adv.*, 2021, **11**, 100066.
- 92 D. M. Yu, S. Yoon, T.-H. Kim, J. Y. Lee, J. Lee and Y. T. Hong, Properties of sulfonated poly(arylene ether sulfone)/electrospun nonwoven polyacrylonitrile composite membrane for proton exchange membrane fuel cells, *J. Membr. Sci.*, 2013, **446**, 212–219.
- 93 B. Swankaert, J. Geltmeyer, K. Rabaey, K. De Buysser, L. Bonin and K. De Clerck, A review on ion-exchange nanofiber membranes: properties, structure and



- application in electrochemical (waste)water treatment, *Sep. Purif. Technol.*, 2022, **287**, 120529.
- 94 D. Archana, J. Dutta and P. K. Dutta, Evaluation of chitosan nano dressing for wound healing: characterization, in vitro and in vivo studies, *Int. J. Biol. Macromol.*, 2013, **57**, 193–203.
  - 95 P. Kallem, N. Yanar and H. Choi, Nanofiber-Based Proton Exchange Membranes: Development of Aligned Electrospun Nanofibers for Polymer Electrolyte Fuel Cell Applications, *ACS Sustainable Chem. Eng.*, 2019, **7**, 1808–1825.
  - 96 R. Takemori, G. Ito, M. Tanaka and H. Kawakami, Ultra-high proton conduction in electrospun sulfonated polyimide nanofibers, *RSC Adv.*, 2014, **4**, 20005–20009.
  - 97 A. M. Samsudin and V. Hacker, PVA/PDDA/Nano-Zirconia Composite Anion Exchange Membranes for Fuel Cells, *Polymers*, 2019, **11**, 1399.
  - 98 E. Passalacqua, F. Lufrano, G. Squadrito, A. Patti and L. Giorgi, Nafion content in the catalyst layer of polymer electrolyte fuel cells: effects on structure and performance, *Electrochim. Acta*, 2001, **46**, 799–805.
  - 99 Y. Sun, Q. Dong, B. Qian, Y. Meng and J. Qiu, Electrolysis removal of methyl orange dye from water by electrospun activated carbon fibers modified with carbon nanotubes, *Chem. Eng. J.*, 2014, **253**, 73–77.
  - 100 Y. Chen, J. A. Wrubel, W. E. Klein, S. Kabir, W. A. Smith, K. C. Neyerlin and T. G. Deutsch, High-Performance Bipolar Membrane Development for Improved Water Dissociation, *ACS Appl. Polym. Mater.*, 2020, **2**, 4559–4569.
  - 101 A. Zaher, W. El Rouby and N. Barakat, Influences of tungsten incorporation, morphology and calcination temperature on the electrocatalytic activity of Ni/C nanostructures toward urea elimination from wastewaters, *Int. J. Hydrogen Energy*, 2020, **45**, 8082–8093.
  - 102 S. N. Banitaba, D. Semnani, E. Heydari-Soureshjani, B. Rezaei and A. A. Ensafi, The effect of concentration and ratio of ethylene carbonate and propylene carbonate plasticizers on characteristics of the electrospun PEO-based electrolytes applicable in lithium-ion batteries, *Solid State Ionics*, 2020, **347**, 115252.
  - 103 S. N. Banitaba and A. Ehrmann, Application of electrospun nanofibers for fabrication of versatile and highly efficient electrochemical devices: a review, *Polymers*, 2021, **13**(11), 1741.
  - 104 Y. Ou, J. Wen, H. Xu, S. Xie and J. Li, Ultrafine LiCoO<sub>2</sub> powders derived from electrospun nanofibers for Li-ion batteries, *J. Phys. Chem. Solids*, 2013, **74**, 322–327.
  - 105 F.-D. Yu, L.-F. Que, C.-Y. Xu, M.-J. Wang, G. Sun, J.-G. Duh and Z.-B. Wang, Dual conductive surface engineering of Li-Rich oxides cathode for superior high-energy-density Li-Ion batteries, *Nano Energy*, 2019, **59**, 527–536.
  - 106 X. Mao, T. Hatton and G. Rutledge, A Review of Electrospun Carbon Fibers as Electrode Materials for Energy Storage, *Curr. Org. Chem.*, 2013, **17**, 1390–1401.
  - 107 M. Wei, M. Jiang, L. Xiaobo, M. Wang and S. Mu, Graphene-doped electrospun nanofiber membrane electrodes and proton exchange membrane fuel cell performance, *J. Power Sources*, 2016, **327**, 384–393.
  - 108 M. Zhi, N. Mariani, R. Gemmen, K. Gerdes and N. Wu, Nanofiber scaffold for cathode of solid oxide fuel cell, *Energy Environ. Sci.*, 2011, **4**, 417–420.
  - 109 K. M. Skupov, I. I. Ponomarev, D. Y. Razorenov, V. G. Zhigalina, O. M. Zhigalina, I. I. Ponomarev, Y. A. Volkova, Y. M. Volkovich and V. E. Sosenkin, Carbon nanofiber paper cathode modification for higher performance of phosphoric acid fuel cells on polybenzimidazole membrane, *Russ. J. Electrochem.*, 2017, **53**, 728–733.
  - 110 A. Jindal and S. Basu, Improvement in electrocatalytic activity of oxygen reduction reaction of electrospun carbon nitride/polyacrylonitrile nanofibers by addition of carbon black and Nafion<sup>®</sup> fillers, *Int. J. Hydrogen Energy*, 2016, **41**, 11624–11633.
  - 111 X. Liu, Z. Yang, Y. Zhang, C. Li, J. Dong, Y. Liu and H. Cheng, Electrospun multifunctional sulfonated carbon nanofibers for design and fabrication of SPEEK composite proton exchange membranes for direct methanol fuel cell application, *Int. J. Hydrogen Energy*, 2017, **42**(15), 10275–10284.
  - 112 J. J. Slack, M. Brodt, D. A. Cullen, K. S. Reeves, K. L. More and P. N. Pintauro, Impact of Polyvinylidene Fluoride on Nanofiber Cathode Structure and Durability in Proton Exchange Membrane Fuel Cells, *J. Electrochem. Soc.*, 2020, **167**, 054517.
  - 113 A. Enrico, W. Zhang, M. Lund Traulsen, E. M. Sala, P. Costamagna and P. Holtappels, La<sub>0.6</sub>Sr<sub>0.4</sub>Co<sub>0.2</sub>Fe<sub>0.8</sub>O<sub>3-δ</sub> nanofiber cathode for intermediate-temperature solid oxide fuel cells by water-based sol-gel electrospinning: synthesis and electrochemical behaviour, *J. Eur. Ceram. Soc.*, 2018, **38**, 2677–2686.
  - 114 S. Chung, D. Shin, M. Choun, J. Kim, S. Yang, M. Choi, J. W. Kim and J. Lee, Improved water management of Pt/C cathode modified by graphitized carbon nanofiber in proton exchange membrane fuel cell, *J. Power Sources*, 2018, **399**, 350–356.
  - 115 R. Mei, J. Xi, L. Ma, L. An, F. Wang, H. Sun, Z. Luo and Q. Wu, Multi-Scaled Porous Fe–N/C Nanofibrous Catalysts for the Cathode Electrodes of Direct Methanol Fuel Cells, *J. Electrochem. Soc.*, 2017, **164**, F1556.
  - 116 S. Kabir, T. Van Cleve, S. Khandavalli, S. Medina, S. Pylypenko, S. Mauger, M. Ulsh and K. C. Neyerlin, Toward Optimizing Electrospun Nanofiber Fuel Cell Catalyst Layers: Microstructure and Pt Accessibility, *ACS Appl. Energy Mater.*, 2021, **4**, 3341–3351.
  - 117 W. Zhang, M. W. Brodt and P. N. Pintauro, Nanofiber Cathodes for Low and High Humidity Hydrogen Fuel Cell Operation, *ECS Trans.*, 2011, **41**, 891.
  - 118 N. A. M. Barakat, M. T. Amen, F. S. Al-Mubaddel, M. R. Karim and M. Alrashed, NiSn nanoparticle-incorporated carbon nanofibers as efficient electrocatalysts for urea oxidation and working anodes in direct urea fuel cells, *J. Adv. Res.*, 2019, **16**, 43–53.
  - 119 M. Abdelkareem, Y. Al Haj, M. Al Ajami, H. Alawadhi and N. Barakat, Ni–Cd Carbon Nanofibers as an Effective Catalyst for Urea Fuel Cell, *J. Environ. Chem. Eng.*, 2017, **6**(1), 332–337.



- 120 Q. Hu, C. Liu, L. Fan, Y. Wang and Y. Xiong, Nanofiber-based  $\text{La}_{0.4}\text{Sr}_{0.6}\text{TiO}_3\text{-Gd}_{0.2}\text{Ce}_{0.8}\text{O}_{1.9}\text{-Ni}$  composite anode for solid oxide fuel cells, *Electrochim. Acta*, 2018, **265**, 1–9.
- 121 G. Yu, T. S. Li, M. Xu, M. Andersson, B. Li, H. Tang, J. Parbey and J. Shao, Fabrication of nickel-YSZ cermet nanofibers via electrospinning, *J. Alloys Compd.*, 2017, **693**, 1214–1219.
- 122 C. Feng, T. Takeuchi, M. A. Abdelkareem, T. Tsujiguchi and N. Nakagawa, Carbon– $\text{CeO}_2$  composite nanofibers as a promising support for a PtRu anode catalyst in a direct methanol fuel cell, *J. Power Sources*, 2013, **242**, 57–64.
- 123 T. Cai, M. Huang, Y. Huang and W. Zheng, Enhanced performance of microbial fuel cells by electrospinning carbon nanofibers hybrid carbon nanotubes composite anode, *Int. J. Hydrogen Energy*, 2019, **44**(5), 3088–3098.
- 124 H.-Y. Jung and S.-H. Roh, Carbon Nanofiber/Polypyrrole Nanocomposite as Anode Material in Microbial Fuel Cells, *J. Nanosci. Nanotechnol.*, 2017, **17**, 5830–5833.
- 125 G. Massaglia, V. Margaria, M. Re Fiorentin, K. Pasha, A. Sacco, M. Castellino, A. Chiodoni, S. Bianco, F. Pirri and M. Quaglio, Nonwoven mats of N-doped carbon nanofibers as high-performing anodes in microbial fuel cells, *Mater. Today Energy*, 2020, **16**, 100385.
- 126 U. Karra, S. S. Manickam, J. R. McCutcheon, N. Patel and B. Li, Power generation and organics removal from wastewater using activated carbon nanofiber (ACNF) microbial fuel cells (MFCs), *Int. J. Hydrogen Energy*, 2013, **38**, 1588–1597.
- 127 I. Mohamed, K. Palsamy, A. S. Yasin, W. Iqbal and C. Liu, Electrochemical impedance investigation of urea oxidation in alkaline media based on electrospun nanofibers towards the technology of direct-urea fuel cells, *J. Alloys Compd.*, 2019, **816**, 152513.
- 128 N. A. Garcia-Gomez, I. Balderas-Renteria, D. I. Garcia-Gutierrez, H. A. Mosqueda and E. M. Sánchez, Development of mats composed by  $\text{TiO}_2$  and carbon dual electrospun nanofibers: a possible anode material in microbial fuel cells, *Mater. Sci. Eng., B*, 2015, **193**, 130–136.
- 129 N. Abdullah, S. K. Kamarudin, L. K. Shyuan and N. A. Karim, Fabrication and Characterization of New Composite  $\text{TiO}_2$  Carbon Nanofiber Anodic Catalyst Support for Direct Methanol Fuel Cell via Electrospinning Method, *Nanoscale Res. Lett.*, 2017, **12**, 613.
- 130 S. Zhang, G. He, X. Gong, X. Zhu, X. Wu, S. Xinye, X. Zhao and H. Li, Electrospun nanofiber enhanced sulfonated poly (phthalazinone ether sulfone ketone) composite proton exchange membranes, *J. Membr. Sci.*, 2015, **493**, 58–65.
- 131 C. Shen, R. Wycisk and P. N. Pintauro, High performance electrospun bipolar membrane with a 3D junction, *Energy Environ. Sci.*, 2017, **10**, 1435–1442.
- 132 M. Ahn, S. Han, J. Lee and W. Lee, Electrospun composite nanofibers for intermediate-temperature solid oxide fuel cell electrodes, *Ceram. Int.*, 2020, **46**, 6006–6011.
- 133 J. Woo Park, R. Wycisk, G. Lin, P. Ying Chong, D. Powers, T. Van Nguyen, R. P. Dowd and P. N. Pintauro, Electrospun Nafion/PVDF single-fiber blended membranes for regenerative  $\text{H}_2/\text{Br}_2$  fuel cells, *J. Membr. Sci.*, 2017, **541**, 85–92.
- 134 J. W. Park, R. Wycisk and P. N. Pintauro, Nafion/PVDF nanofiber composite membranes for regenerative hydrogen/bromine fuel cells, *J. Membr. Sci.*, 2015, **490**, 103–112.
- 135 S. Shahgaldi, M. Ghasemi, W. R. Wan Daud, Z. Yaakob, M. Sedighi, J. Alam and A. F. Ismail, Performance enhancement of microbial fuel cell by PVDF/Nafion nanofibre composite proton exchange membrane, *Fuel Process. Technol.*, 2014, **124**, 290–295.
- 136 K. Vezzù, G. Nawn, E. Negro, G. Crivellaro, J. W. Park, R. Wycisk, P. N. Pintauro and V. Di Noto, Electric Response and Conductivity Mechanism of Blended Polyvinylidene Fluoride/Nafion Electrospun Nanofibers, *J. Am. Chem. Soc.*, 2020, **142**, 801–814.
- 137 J. J. Slack, C. Gumezi, N. Dale, J. Parrondo, N. Macauley, R. Mukundan, D. Cullen, B. Sneed, K. More and P. N. Pintauro, Nanofiber Fuel Cell MEAs with a PtCo/C Cathode, *J. Electrochem. Soc.*, 2019, **166**, F3202–F3209.
- 138 A. Jindal, S. Basu, N. Chauhan, T. Ukai, D. S. Kumar and K. T. Samudhyatha, Application of electrospun  $\text{CN}_x$  nanofibers as cathode in microfluidic fuel cell, *J. Power Sources*, 2017, **342**, 165–174.
- 139 M. Zhi, S. Lee, N. Miller, N. H. Menzler and N. Wu, An intermediate-temperature solid oxide fuel cell with electrospun nanofiber cathode, *Energy Environ. Sci.*, 2012, **5**, 7066–7071.
- 140 E. Zhao, C. Ma, W. Yang, Y. Xiong, J. Li and C. Sun, Electrospinning  $\text{La}_{0.8}\text{Sr}_{0.2}\text{Co}_{0.2}\text{Fe}_{0.8}\text{O}_{3-\delta}$  tubes impregnated with  $\text{Ce}_{0.8}\text{Gd}_{0.2}\text{O}_{1.9}$  nanoparticles for an intermediate temperature solid oxide fuel cell cathode, *Int. J. Hydrogen Energy*, 2013, **38**, 6821–6829.
- 141 M. Ahn, J. Cho and W. Lee, One-step fabrication of composite nanofibers for solid oxide fuel cell electrodes, *J. Power Sources*, 2019, **434**, 226749.
- 142 I. I. Ponomarev, K. M. Skupov, D. Y. Razorenov, V. G. Zhigalina, O. M. Zhigalina, I. I. Ponomarev, Y. A. Volkova, M. S. Kondratenko, S. S. Bukalov and E. S. Davydova, Electrospun nanofiber pyropolymer electrodes for fuel cells on polybenzimidazole membranes, *Russ. J. Electrochem.*, 2016, **52**, 735–739.
- 143 S. Uhm, B. Jeong and J. Lee, A facile route for preparation of non-noble CNF cathode catalysts in alkaline ethanol fuel cells, *Electrochim. Acta*, 2011, **56**, 9186–9190.
- 144 Q. Hu, L. Fan, Y. Wang, Z. Wang and Y. Xiong, Nanofiber-based  $\text{La}_x\text{Sr}_{1-x}\text{TiO}_3\text{-Gd}_y\text{Ce}_{1-y}\text{O}_{2-\delta}$  Composite Anode for Solid Oxide Fuel Cells, *Ceram. Int.*, 2017, **43**(15), 12145–12153.
- 145 K.-R. Lee, C.-J. Tseng, J.-K. Chang, K.-W. Wang, Y.-S. Huang, T.-C. Chou, K.-C. Chiu, L. D. Tsai and S.-W. Lee,  $\text{Ba}_{1-x}\text{Sr}_x\text{Ce}_{0.8-y}\text{Zr}_y\text{O}_{2.2-\delta}$  protonic electrolytes synthesized by hetero-composition-exchange method for solid oxide fuel cells, *Int. J. Hydrogen Energy*, 2017, **42**(34), 22222–22227.
- 146 W. Li, Y. Cheng, Q. Zhou, T. Wei, Z. Li, H. Yan, Z. Wang and X. Han, Evaluation of double perovskite  $\text{Sr}_2\text{FeTiO}_{6-\delta}$  as potential cathode or anode materials for intermediate-temperature solid oxide fuel cells, *Ceram. Int.*, 2015, **41**(9), 12393–12400.
- 147 B. M. Thamer, M. H. El-Newehy, N. A. M. Barakat, M. A. Abdelkareem, S. S. Al-Deyab and H. Y. Kim, Influence



- of Nitrogen doping on the Catalytic Activity of Ni-incorporated Carbon Nanofibers for Alkaline Direct Methanol Fuel Cells, *Electrochim. Acta*, 2014, **142**, 228–239.
- 148 M. F. R. Hanifah, J. Jaafar, M. H. Othman, A. Ismail, M. Rahman, N. Yusof and F. Aziz, Electro-spun of novel PVDF-Pt-Pd/RGO-CeO<sub>2</sub> composite nanofibers as the high potential of robust anode catalyst in direct methanol fuel cell: fabrication and characterization, *Inorg. Chem. Commun.*, 2019, **107**, 107487.
  - 149 Y. Ito, T. Takeuchi, T. Tsujiguchi, M. A. Abdelkareem and N. Nakagawa, Ultrahigh methanol electro-oxidation activity of PtRu nanoparticles prepared on TiO<sub>2</sub>-embedded carbon nanofiber support, *J. Power Sources*, 2013, **242**, 280–288.
  - 150 H. Wu, T. Yuan, Q. Huang, H. Zhang, Z. Zou, J. Zheng and H. Yang, Polypyrrole nanowire networks as anodic microporous layer for passive direct methanol fuel cells, *Electrochim. Acta*, 2014, **141**, 1–5.
  - 151 Y. Zheng, Z. Zhang, X. Zhang, H. Ni, Y. Sun, Y. Lou, X. Li and Y. Lu, Application of Pt-Co nanoparticles supported on CeO<sub>2</sub>-C as electrocatalyst for direct methanol fuel cell, *Mater. Lett.*, 2018, **221**, 301–304.
  - 152 J. Park, R. Wycisk, G. Lin, P. Chong, D. Powers, T. Nguyen, R. Dowd and P. Pintauro, Electrospun Nafion/PVDF Single-fiber Blended Membranes for Regenerative H<sub>2</sub>/Br<sub>2</sub> Fuel Cells, *J. Membr. Sci.*, 2017, **541**, 85–92.
  - 153 J. Ballengee and P. Pintauro, Preparation of nanofiber composite proton-exchange membranes from dual fiber electrospun mats, *J. Membr. Sci.*, 2013, **442**, 187–195.
  - 154 J. Park, R. Wycisk and P. Pintauro, Nafion/PVDF Nanofiber Composite Membranes for Regenerative Hydrogen/Bromine Fuel Cells, *J. Membr. Sci.*, 2015, **490**, 103–112.
  - 155 J. W. Park, R. Wycisk, P. N. Pintauro, V. Yarlagadda and T. Van Nguyen, Electrospun Nafion<sup>®</sup>/polyphenylsulfone composite membranes for regenerative hydrogen bromine fuel cells, *Materials*, 2016, **9**(3), 143.
  - 156 K. Vezzù, G. Nawn, E. Negro, G. Crivellaro, J. W. Park, R. Wycisk, P. N. Pintauro and V. Di Noto, Electric Response and Conductivity Mechanism of Blended Polyvinylidene Fluoride/Nafion Electrospun Nanofibers, *J. Am. Chem. Soc.*, 2020, **142**, 801–814.
  - 157 T. Tamura and H. Kawakami, Aligned electrospun nanofiber composite membranes for fuel cell electrolytes, *Nano Lett.*, 2010, **10**, 1324–1328.

